Glacial dynamics in Prealpine narrow valleys during the Last Glacial Maximum inferred by lowlands fluvial record (NE Italy)

Sandro Rossato[1], Anna Carraro[2], Giovanni Monegato[2], Paolo Mozzi[1], Fabio Tateo[2]

[1]Department of Geosciences, University of Padova, 35131, Italy
[2]Institute of Geosciences and Earth Resources (IGG) – National Research Council (CNR), Padova, 35131, Italy

Correspondence to: Sandro Rossato (sandro.rossato@unipd.it)

Abstract. During the Last Glacial Maximum (LGM), most of the major glaciated basins of the European Southern Alps had piedmont lobes with large outwash plains; only few glaciers remained within the valley. The formers left well-preserved terminal moraines, whose investigation allowed to infer their evolution and chronology. Valley glaciers remnants, on the contrary, are often scantly preserved and changes can be detected only through the correlation with the glaciofluvial deposits in downstream alluvial basins. The Brenta glacial systems dynamics in its terminal tract was inferred through a wide range of sediment analysis techniques on an alluvial stratigraphic record of the Brenta megafan (NE Italy) and the mapping of in-valley glacial/glaciofluvial remnants. Glaciers flowing across narrow gorges turned out to be possibly slowed/blocked by such morphology and glacial/sediment fluxes being diverted to lateral valleys. Moreover, narrow valleys may induce glaciers to bulge and form icefalls at their front, preventing the formation of terminal moraines. The Brenta glacier was probably slowed/blocked by the narrow Valsugana gorge downstream of Primolano and was effectively diverted eastwards across a windgap (Canal La Menor valley), joining the Cismon/Piave glaciers near Rocca and ending ~2 km downstream. The Cismon and Piave catchments started to contribute to the Brenta system right after 27 ka cal BP up to at least ~19.5 ka cal BP. After the glaciers collapse the Piave River flowed again into its main valley, whilst the Cismon continued to merge with the Brenta. Our investigation shows that glacial catchments may significantly vary over time during a single glaciation in rugged Alpine terrains. Sand petrography and chemical/mineralogical composition of sediments are good tracer of such variations, that reflect in the glacial and glaciofluvial systems and can be recognized in the alluvial stratigraphic record far downstream from the glacier front.

1 Introduction

Mountain glaciers are complex systems, whose evolution affects both their mountain basins and the alluvial plains that receive the glaciofluvial water-and-sediment flux (e.g. Russell et al., 2006). Few minor valley glaciers are currently present in the highest areas of the European Alps (Evans, 2006), whereas during Pleistocene glaciations large ice-streams flowed along most of the Alpine valleys, leading to deep landscape modifications (e.g. Koppes and Montgomery, 2009; Preusser et al., 2010; Wirsig et al., 2016). Most of the major glaciated basins had piedmont lobes with large outwash plains, where the stratigraphic

reconstruction and available chronology allowed to infer the evolution of the glacial system (Monegato et al., 2007; Preusser et al., 2011; Ravazzi et al., 2012; Fontana et al., 2014). However, there are catchments whose glacier remained within the valley and their evolution could be detected through the correlation with the related glaciofluvial deposition in the piedmont area (van Husen and Reitner, 2011; Rossato et al., 2013).

The Last Glacial Maximum (LGM) was the last cold extreme on Earth and it provided the best-preserved sedimentary and geomorphic record among all Pleistocene glaciations (Bowen, 2009; Clark et al., 2009; Hughes and Gibbard, 2015). In Europe, the Alps and their foreland constitute a key region for LGM studies, as evidence of this event is widespread and chronologically well framed between 30 and 17.5 ka cal BP (e.g., Ivy-Ochs et al., 2008; Ivy-Ochs, 2015; Rossato and Mozzi, 2016; Monegato et al., 2017). Moreover, they constitute an effective barrier for wind circulation (Florineth and Schlüchter, 2000; Luetscher et al., 2015) and offer the unique opportunity to validate climate models (e.g. Smiatek et al., 2009; Torma et al., 2015) and study how glacial processes affect mountain chains (e.g. Norton et al., 2010). LGM glaciers were filling the valleys fed by the major accumulation zones located in the axial and highest part of the Alps (e.g., van Husen, 1987; Kelly et al., 2004; Wirsig et al., 2016). In the southern alpine sector, due to different wind circulation regime (Luetscher et al., 2015) topography greatly influenced glacier evolution (Wirsig et al., 2016). Alpine glaciers and their sedimentary outputs proved to react differently to climatic signals, both along the north-south (e.g. Luetscher et al., 2015) and the west-east directions (Becker et al., 2016; Monegato et al., 2017; Seguinot et al., 2017). Differences arise also when dealing with neighboring glacial systems, due to their size, catchment topography and possible glaciers confluences and transfluences (e.g., Kelly et al., 2004; Monegato et al., 2007; Rossato et al., 2013).

The present availability of a wide range of proxies, coupled with the increased accuracy of geochronological methods (Brauer et al., 2014), allow for a better assessment of LGM glaciers' behavior compared to earlier studies in the Alps, mostly based on landforms and deposits characterization (e.g. Penck and Brückner, 1909; Sacco, 1937; Venzo et al., 1977; Schlüchter, 1986; van Husen, 1987). The analysis of loess and palaeosols has been coupled with biological proxies, such as pollen, chironomids, charcoal and many more (e.g., Heiri et al., 2014; Samartin et al., 2016). Petrographic/mineralogical study of sediments have supported palaeoenvironmental reconstructions and allowed to infer variations in the sedimentary systems (Garzanti et al., 2011).

In this paper we investigate the interaction between the LGM glaciers in the middle Brenta valley (also known as "Valsugana", Italian Forealps) and the related glaciofluvial system in the piedmont plain (Fig. 1). During the LGM, the Brenta glacial system received contribution from the major Adige (Etsch) glacier (Trevisan, 1939; Tessari, 1973; Avanzini et al., 2010; Rossato et al., 2013), and fed a fluvial megafan, which is one of the most prominent sedimentary alluvial systems on the southern side of the Alpine chain (Mozzi, 2005; Fontana et al., 2014). The main aim of this paper is to explore and define the possibility of correlating glacial advances and transfluences in mountain areas with sedimentation pulses in the lowlands using integrated geomorphic, sedimentary, petrographic, mineralogical, geochemical and geochronological evidence.

2 Setting

The Venetian Forealps are geologically detached from the Dolomites by the Valsugana fault (Castellarin et al., 2006) and are characterized by a belt of carbonate plateaus deeply carved by the lower reaches of the Astico, Brenta, Cismon and Piave valleys (Fig. 1). Except for the Astico River, whose catchment is restricted to the western part of the Venetian Forealps, the others have their upper catchments in the Dolomites, which include the Permo-Triassic sedimentary successions (sandstones, dolostones, limestones and volcanic rocks), the low-grade metamorphic basement and the Permian porphyries (e.g., Bartolomei et al., 1969; Avanzini et al., 2010; Fig. 1). The Brenta and Cismon catchments also include the Permian plutonic rocks of Cima d'Asta (Fig. 1). In the footwall of the Valsugana Fault the Jurassic-Tertiary sedimentary succession crops out, including different types of limestones, turbiditic sequences and the terrigenous units of the Southalpine foredeep (e.g., Massari et al., 1986; Barbieri and Grandesso, 2007; Stefani et al., 2007). In particular, in the Cismon catchment, all around Lamon (Fig. 1), micritic limestones crop out extensively (Tessari, 1973). Here, a remarkable fluvial aggradation took place during/after deglaciation, later followed by river incision and the formation of a terrace staircase, the highest and largest terrace being located at about 600 m a.s.l., 200 m above the Cismon valley bottom. The deposition of such an amount of sediment was probably due to the damming of the Cismon valley south of Lamon, possibly by a large dead-ice mass or a landslide event, but no direct evidence of it has been found (Tessari, 1973).

The plateaus characterizing the Venetian Forealps (Castiglioni et al., 1988) have mean elevations from 900 to 2000 m a.s.l. and hosted small cirque or plateau glaciers during the last glaciation (Trevisan, 1939; Carraro and Sauro, 1979; Baratto et al., 2003; Barbieri and Grandesso, 2007). The major Astico (Cucato, 2001; Rossato et al., 2013) and Piave (Venzo, 1977; Carton et al., 2009) valleys were carved by ice-streams that reached the lower valley reaches and left well-preserved terminal moraines (Fig. 1). Despite the large megafan ascribed to the LGM (Mozzi, 2005; Fontana et al., 2008; Rossato and Mozzi, 2016), the Brenta glacier is the only major system in the south-eastern Alps that left no clear evidence of terminal moraines (Castiglioni, 2004). The reason why the Brenta system did not follow such evolutionary path remains unresolved, although some early authors already dealt with this challenging topic (e.g. Taramelli, 1882; Penck and Brückner, 1909; Castiglioni, 1940). Taramelli (1882) and Castiglioni (1940) placed the Brenta glacier front near the town of Valstagna, about 10.5 km south of the confluence between the Brenta and Cismon valleys (Fig. 1), while Penck and Brückner (1909) located it about 6 km further to the south, near the town of Solagna. Due to the lack of direct geomorphic or sedimentary evidence of the glacier's front, both interpretations were based on the speculation that the glacier thinned gradually downstream of the last preserved lateral moraine at Enego (elevation 790-760 m a.s.l.). The terminal tract of the Cismon valley, named Corlo valley, was closed by a dam in 1953 and filled by the artificial Corlo Lake (Fig. 1), so no further survey is presently possible.

The Brenta fluvial megafan is part of the foreland basin of the uplifting Eastern Southalpine chain (e.g., Castellarin et al., 2006; Stefani et al., 2007). This megafan extends from the Brenta valley mouth to the present Venetian coastline. It can be roughly separated into two sectors: i) piedmont (~20 km from the apex), made of gravel and with an average topographic gradient of

3-5‰, ii) low plain, made of sandy fluvial ridges and silty-clayey floodplain, with a decreasing of topographic gradient to less than 1‰ (Mozzi, 2005; Fontana et al., 2008; Mozzi et al., 2013).

3 Methods

This investigation was carried out through field survey, coring, petrographic and mineralogical analyses and remote sensing. All methods and results are presented independently, whilst their meaning, implications and interconnections are discussed thereafter.

3.1 Field survey

An extensive mapping of the Quaternary sediments cropping out in the area of the middle Valsugana and the junctions with Canal La Menor and lower Cismon (Corlo) valley, was performed (Fig. 2). Sedimentary facies were observed and described in the outcrops to identify their original depositional setting; particular attention was devoted to the lithology of the clasts, which provided information on the provenance of the sediments. In this perspective, the geology of the eastern Southern Alps (Fig. 1) allows a clear distinction of each drainage basin with different petrographic signatures. Porphyries, granites and metamorphic rocks (i.e. Permian volcanic rocks, Lower Permian plutonic rocks and pre-Permian Varisican basement in Fig. 1, respectively) are indicators of Brenta and Cismon valleys and, thanks also to their high resistance to weathering, can help in identifying glacial deposits upon a carbonate bedrock.

Relevant landforms were accurately surveyed, with particular attention to the LGM moraines which are generally well preserved and quite easily identifiable in these areas, where little anthropogenic activity took place.

3.2 Cores

Two 30-m-long cores were drilled near the city of Piazzola sul Brenta, in the upper part of the Brenta megafan, about five km apart and at a topographic elevation of about 30 m a.s.l. (Fig. 3). These cores were part of a pilot study on groundwater geochemistry (Carraro et al., 2013; 2015). They were described basing on the lithofacies of the sediments and sampled for sand petrography and mineralogical analyses. Five organic samples were collected from the inner part of the cores to minimize contamination and dated with the ^{14}C AMS method at the radiocarbon laboratory of the University of Zurich (Switzerland) (Table 1). OxCal software (version 4.2, Bronk Ramsey, 2009; IntCal13 calibration curve, Reimer et al., 2013), has been used to calibrate laboratory ages.

A single hand-core was drilled in the Guarda area, on the northern flank of the Canal La Menor valley, uphill of an elongated ridge that has been identified as a LGM lateral moraine (see Results chapter and Fig. 2 for location), at about 660 m a.s.l.. This borehole has been realized with a hand-auger (Edelman combination type, Ejikelkamp^{TM}); this equipment allows to obtain a semi-disturbed sequence of fine sediments, with the limitation that the maximum grain size of the sediments that can be sampled is coarse sand to fine gravel.

3.3 Sand petrography

Ten samples were collected from the two long cores for provenance analysis. The entire sand fraction was isolated and impregnated in an epoxy resin according to Gazzi et al. (1973) methodology, to obtain samples for thin-section analysis comparable with river endmembers after Garzanti et al. (2006) and Monegato et al. (2010). These were subsequently stained with alizarine-red solution for the determination of the carbonate phases. Following the Gazzi-Dickinson method 400 points per thin section were counted using a 0.5 mm grid spacing (Ingersoll et al., 1984). Data and parameters were reported in Table 2 and plotted in ternary diagrams.

Principal component analysis (PCA) was performed using CoDaPack (Comas and Henestrosa, 2011) using the compositional biplot (Aitchinson and Greenacre, 2002) for better visualizing the dataset and the variables . The ternary diagrams with the most representative variables are proposed to discuss the data structure. The centering (e.g., Buccianti et al., 1999; von Eynatten et al., 2002) was used for avoiding disturbances related to the dominance of one or two components. In the statistical analysis, petrofacies of modern rivers (Garzanti et al., 2006; Monegato et al., 2010) were included for comparison in order to assess the sediment provenance in the different stratigraphic intervals.

In addition, the statistical technique by Vezzoli and Garzanti (2009) was also adopted to assess the contribution of major drainage systems of the area related to the Brenta, Cismon and Piave rivers (Fig. 1) as endmembers. The parameters were compared to evaluate the possible matching with these catchments and results with R^2 >0.7 were considered robust. Except for one sample (RB1-8), all the samples show a good interpretation confidence (Tab. 2).

3.4 X-ray diffraction (XRD)

In order to minimize preferred orientation, samples were pulverized and backloaded. A Philips X'Pert Pro diffractometer (Cu tube and secondary monochromator) was adopted. The mineral constituents were quantified using HighScore plus software following Rietveld refinement (Young, 1993); zincite (ZnO) was added as an internal standard (sample:standard = 10:1 weight ratio). It allows also to estimate the amorphous components (labelled Am.XRD, in Stab. 1).

To check the reliability of mineral quantification, the chemical composition of samples was calculated using stoichiometric mineral composition (for quartz, calcite, dolomite, feldspars, illite and kaolinite); a Fe-rich, Mg-poor dolomite was also included in the calculation (according to the XRD evidence of non-stoichiometric dolomite in almost all the samples), two Al-chlorites (Fe- or Mg-enriched) and organic matter. The comparison between calculated and measured chemical composition was considered satisfactory (total least square within 10 for 29 samples over 32).

3.5 Chemical composition

The major elements, some trace elements (including N) and the organic carbon (C_{org}) were determined as reported by Carraro et al. (2015). Sample were digested with concentrated HNO_3 + HCl + HF at 140 °C for 90 minutes, then rinsed with H_3BO_3

and heated at 140 °C for 60 minutes. Afterwards, the solutions were analyzed by inductively coupled plasma (ICP-OES) and atomic absorption spectroscopy (AAS). The loss on ignition (LOI) was measured after heating the sample to 860 °C for 20 minutes and to 980 °C for 2 hours.

An automatic elemental analyzer was used to obtain C_{org} and total N for the carbonate-free residues. The measures were repeated at least twice using Ag sample containers.

All the mineralogical and chemical data were used for hierarchical cluster analysis (SPSS), in order to point out sample similarities and/or anomalies. Five dark sediments were grouped in the same cluster; this group is characterized by a percentage of organic matter higher than 12 %. This threshold value was used for peat identification (see Carraro et al., 2015 for analytical details). Macroscopic features (black color and fine-grained) were used for peat identification when chemical data were not available.

3.6 Remote sensing

Aerial photographs and satellite images of public use (Google Earth and Bing databases) were processed and analyzed for the mapping of relict landforms. Panoramic and detail photos were acquired during field surveys and subsequently used in conjunction with the other images.

A Digital Elevation Model (DEM) provided by the Veneto Region, based on topographic data derived from 1:5000 topographic maps (5 m cell-size; XY accuracy: 2 m - http://idt.regione.veneto.it/app/metacatalog/) was used. It covers the entire study area, assuring a uniform accuracy of investigation. The various DEM tiles were assembled with ArcGis (10.4.1 version) to better process them and to obtain a uniform visualization. All topographic profiles here presented were based on this DEM.

4 Results

4.1 Field survey

The field survey allowed to identify some key stratigraphic sections and outcrops that were regarded to be representative of specific sectors of the study area (see Fig. 2 for location). Their descriptions are presented here in geographical order, from east to west and from north to south.

4.1.1 “Seren valley” and “Roncon” outcrops

In the Seren valley bottom (390 m a.s.l.), widespread outcrops of matrix-supported diamicton can be found (Fig. 2). These deposits are overconsolidated and characterized by centimetric clasts with sparse boulders, sub-rounded to angular in shape, embedded in abundant silty matrix. In the thalweg of the Stizzone Creek that runs along the valley, silty matrix-supported diamicton crops out, with striated clasts. Different sedimentary, volcanic and metamorphic lithologies are present in the deposit, all showing no evident weathering. The Seren valley deposits can be ascribed to melt-out tills, whilst those located

along the thalweg are lodgment till, both belonging to the Piave glacier. In the nearby Roncon section (Fig. 2), a deposit similar to these melt-out tills could be observed in few, decametric outcrops at an elevation of about 450 m a.s.l..

4.1.2 "Monache" ridges

In the Monache plateau a series of ridges, more than 0.5 km long, is present at elevation ranging from 750 to 650 m a.s.l. (Fig. 2). These ridges are elongated and asymmetric in shape, as they present a very steep, 3 to 20 m high downhill flank, whilst the uphill side is lower and consists of a low-angle slope that rests on the bedrock. These landforms consist mainly of matrix-supported diamicton characterized by white/grey limestone clasts, up to 50 cm large, with dark flint nodules (black and brown). All observed clasts are made of "Maiolica" limestone, a Lower Cretaceous formation that crops out extensively on the whole Grappa Massif (Dal Piaz et al., 1946; Carraro et al. 1989), where the ridges are located. These ridges are interpreted as lateral moraines of the Piave glacier fed by local limestones debris.

4.1.3 "Guarda" ridge and core

The Guarda ridge is located on the northern side of the Canal La Menor valley, in the Casere alla Guarda locality, at an elevation ranging from 700 to 660 m a.s.l. (Fig. 2). It is about 400 m long, up to 30 m high and has very steep flanks. This ridge consists of a polygenic diamicton with clasts of porphyry, limestone and siltstone, up to 50 cm in size, sub-rounded to angular in shape. Weathering of clasts is minimal, and the material is not overconsolidated. It is interpreted as a lateral moraine of the tongue of the Brenta glacier that was flowing through the Canal La Menor valley.

A 4.7-m long core (Guarda1 core) was drilled manually in the Guarda locality, at an elevation of 664 m a.s.l., on a wide valley bottom that is closed downstream by the Guarda moraine (Fig. 3 and 6). The cored sequence consists of clayey silt layers, grey in color, with sporadic presence of centimetric sandy intervals. A single 30-cm-thick gravelly layer is present between 3.2 and 3.5 m b.s., with sparse angular gravel clasts (3-4 mm in size) immersed in sandy matrix. The Guarda1 core testifies a phase of low-energy sedimentation in a confined environment, with a single high-energy event. According to the lack of deep weathering of the deposit and the presence of a poorly-developed soil on top of the succession, the whole sequence is likely to have deposited in a fluvio-lacustrine basin during the late stages of LGM and/or during the Lateglacial and early Holocene, when the Guarda moraine was blocking the runoff from this lateral valley to the main Canal La Menor valley.

4.1.4 "Novegno" and "Col del Gallo" deposits

The top of the Novegno plateau is characterized by a low-gradient plateau at elevations ranging from about 720 to 600 m a.s.l.. In this area, many elongated ridges were found, locally merging one into the other, with a general SW-NE direction (Fig. 2). They are up to 2-km long, 50-m wide and 40-m high, usually with steep slopes. The observed outcrops show that these ridges have polygenic clast composition, being constituted by matrix-supported diamicton with clasts of porphyry, limestone and siltstone, up to 40 cm in size, sub-rounded to angular in shape (Fig. 4b). Between the ridges, as well as on the northern and southern sides of Col del Gallo (780-600 m a.s.l.), scattered patches of similar deposits can be found, characterized by a slightly

higher matrix content (Fig. 2, 4c). The deposit is not over-consolidated and the weathering is minimal. Locally, some big boulders, up to 1.5-m large, were found; these are mainly of porphyry (Fig. 4a) and granite. These sediments can be classified as glacial in origin, more specifically melt-out and flow tills.

On top of Col del Gallo (870 m a.s.l.), no proper outcrops are present, but centimetric clasts of volcanic and metamorphic phyllites were found in the surface soil.

All evidence shows that the Novegno plateau is occupied by many lateral moraines formed by a glacier which was collecting material from an area located at least 25 km to the north, where the nearest outcrops of porphyry can be found (Fig. 1). Similar glacial sediments are found on the northern and southern sides of Col del Gallo (Fig. 4c). It is likely that they relate to the same glacier. The deposits located on top of Col del Gallo are about 100 m higher than the others and may possibly be related to a previous glacial advance.

4.1.5 "Sorist" ridges

In the Sorist mount area a series of at least three ridges, more than 0.8 km long, is present, at an elevation ranging from 760 to 650 m a.s.l. (Fig. 2). These ridges are elongated and present steep flanks, up to 10 m high. Locally the deposits forming these landforms crop out, showing a polygenic nature, with clasts of porphyry, limestone and siltstone, up to 60 cm in size, sub-rounded to angular in shape, embedded in abundant matrix (Fig. 4d). Weathering of clasts is minimal, and the material is not overconsolidated. Some large porphyry boulders, up to 1 m size, are found.

These ridges are interpreted as left moraines of the LGM Brenta glacier, which was flowing through the Valsugana valley.

4.1.6 "Enego" ridge

This 1-km long and more than 70-m high ridge is located on the western side of the Brenta valley, at elevation 790-760 m a.s.l., where the Enego village lies (Fig. 2). This ridge is a lateral moraine of the Brenta glacier, already described by former scholars (Trevisan, 1939; Dal Piaz et al., 1946) and considered to have formed during the LGM. These deposits are the southernmost known Brenta glacier deposits. During our survey, no large boulders (>1 m) were discovered, but a second, smaller ridge was found at lower elevation (~650 m a.s.l.).

These ridges are interpreted as the right-lateral moraines of the Brenta glacier during the LGM.

4.1.7 "Coste" and "Valstagna" sections

In the Coste area, at the bottom of the Valsugana valley on its western side, about 600 m south of the Enego ridge, a stratigraphic section was observed at the excavation front of a gravel pit (Fig. 5), with the base at about 210 m a.s.l. (~10 m above the present valley bottom) (Fig. 2). The section is about 50 m high, 100 m long and it is composed by two main units, here described:

Lower unit: this unit consists of a 10-15 m thick gravel body rich in sandy matrix, presenting cross-to-planar stratification. Clasts are centimetric in size (maximum diameter is about 30 cm), sub-rounded to sub-angular and consist mainly of carbonate

rocks (limestones/marlstones), with abundant siltstones and some granites and porphyries. The lower boundary of this unit is not visible due to the covering by loose debris. The upper boundary with the "upper unit" shows the interfingering of the two units in the western part of the section, near the foot of the rock wall that constitutes the valley side.

Upper unit: from the top of the lower unit up to the topographic surface there is a sedimentary body made of angular clasts, centimetric-to-decimetric in size, with sandy matrix and scattered boulders (maximum diameter is about 1 m). This unit is crudely stratified, with bedding dipping 25-30 degrees towards the valley axis. Clasts are lithologically homogeneous, consisting only of the local carbonate rocks of the overlying rock walls.

The lower unit is attributed to fluvial deposition by the Brenta River, interfingered and superimposed by scree deposits falling from the overlying rock walls.

A similar succession was found on the eastern side of the Brenta valley, in front of the town of Valstagna, about 9 km south of Coste section. Here, a 15-m-high outcrop has been exposed by quarry activity and testify the occurrence of Brenta River fluvial deposits at elevation ~165 to 170 m a.s.l., covered by 10 m of slope deposits.

4.1.8 "Rocca" deposits

About 1 km north of the village of Rocca, two 20-m-high ridges are present, the top being at 310 m a.s.l. (Fig. 2). The northernmost one is made of sub-rounded polygenic matrix-supported diamicton with clasts up to 20 cm, sub-rounded to angular in shape. These ridges are interpreted as frontal moraines of a glacier tongue flowing into the Canal La Menor valley.

The town of Rocca is built upon carbonate bedrock, but a small patch of sediments crops out next to the local graveyard (Fig. 2). This deposit is made of a matrix-supported diamicton with sub-rounded clasts, up to 30 cm large, sub-rounded to angular in shape. Clasts are minimally weathered and mainly carbonate, but porphyry clasts are present as well. The abundant matrix is mainly constituted by sandy particles.

These deposits are interpreted as LGM till deposited by a glacier tongue flowing into the Corlo valley, where the artificial lake is currently located.

4.2 Remote sensing

Whilst investigation of aerial and satellite images was not very profitable, due to the dense vegetation coverage, the DEM provided very valuable data. The DEM allowed to trace laterally those landforms already recognized in the field in few scattered spots, as in the case of the Enego moraine, and to map other new landforms, basing on morphological similarity. In particular, many moraines belonging to the Novegno group have been mapped using this approach. In the geomorphological sketch (Fig. 2), landforms recognized directly on the field are mapped with bright colors, whilst those mapped on the DEM have fainter shades.

4.3 Alluvial plain cores

Cores are here described as lithofacies assemblages, from the bottom up. The depth of the various layers is referred to the top of the core and indicated with the acronym "b.s." (below surface). Detailed logs are presented in Fig. 6. Data concerning the samples collected for radiocarbon dating are summarized in Table 1; see the specific core description for details on the position of the samples in the stratigraphy.

4.3.1 RB1 core

This borehole was drilled in the Brenta megafan near the town of Carturo, about 5 km north of Piazzola sul Brenta (see Fig. 3 for location, Fig. 6 for stratigraphic log), at a topographic elevation of 30 m a.s.l..

The basal part of the core is made of an alternation of sand bodies and silty and clayey layers with varying sand content. The sand is normally well sorted, being constituted at maximum by grains 0.5 mm wide. Six thin (6-18 cm thick) very fine-grained intervals characterized by high organic content are present. Three of them, almost equally spaced (27.5, 21.8 and 9.3 m b.s.) were radiocarbon dated to 26.6-27.3, 25.7-26.1 and 22.6-23.2 ka cal BP, respectively.

At about 9 m b.s. a clear erosional surface is present, marked by an abrupt transition from clayey silt to a coarsening-upward sequence from medium sand to coarse gravel, sub-angular to sub-rounded (largest clasts are about 2 cm). A single, 15 cm-thick silty layer interrupts this succession at 7.85 m b.s.. The uppermost 2.5 m of the core are constituted by a fining upward sequence of sandy and silty layers. No clear evidence of the modern soil has been found at the top.

The core is interpreted as sandy proximal overbank deposits, intercalated with more distal overbank fines indicative of low-energy floodplain deposition. Locally, some intra-ridges swampy areas developed, inducing the formation of peat layers where organic deposition prevailed over minerogenic contribution, as it was common in the south-eastern alpine piedmont during LGM (Miola et al., 2006; Rossato and Mozzi, 2016). The coarsening-upward sequence is ascribable to sandy-gravelly channel sediments that eroded the older deposits at the end of the LGM forming fluvial incised valleys through the whole Brenta megafan (Mozzi et al., 2013). Finally, the top of the core consists of lower-energy channel deposits or proximal overbank sandy and silty fines.

4.3.2 PM1 core

This core was drilled near the town of Piazzola sul Brenta, about 1 km to the west, at an elevation of 27 m a.s.l. (see Fig. 3 for location, Fig. 6 for stratigraphic log).

The entire core is quite homogeneous, being composed by an alternation of silty layers, with a variable content in clay and sand, interbedded with fine sand intervals. The sand is normally well sorted, being constituted at maximum by grains 0.5 mm large. Two layers of medium sand located at 19-20 and 16.3-17.2 m b.s. are the only exception to this rather monotonous sequence. Three thin (10 cm maximum) layers with a very high organic content are present in the uppermost 15 m of the succession, two of which have been radiocarbon dated to 23.2-23,7 (13.45 m b.s.) and 19.9-20.4 (9 m b.s.) ka cal BP,

respectively. The topmost 2 m of the core show evidence of a well-developed soil, constituted by pedogenic horizons C, Bk and Bw, from the bottom up. The entire sequence is topped by a 0.5-m thick anthropogenic landfill made of gravels with silty matrix.

As in the core RB1, the whole sequence can be interpreted as sandy proximal overbank sediments intercalated with finer floodplain deposits. Locally, peat deposition took place when minerogenic contribution was very low, as it occurred also in RB1 core. The topmost soil has characteristic calcic horizons (Calcisol after FAO, 1998), that allow its correlation to the "caranto paleosol", that developed on top of the LGM deposits in the whole Venetian area (Mozzi et al., 2003; ARPAV, 2005; Donnici et al., 2011).

4.4 Sand petrography

The results of the petrographic analysis of the sand fraction, and related statistic, of the two cores RB1 and PM1 are reported in Table 2 and Figure 7. According to the distribution in the biplot diagram (Fig. 7a) samples clustered in different sectors allow to distinguish two petrofacies (A and B), with a single sample (RB1-8) clearly separating towards a carbonaticlastic composition.

Samples related to petrofacies A belong to the RB1 core below the peat layer at 27.5 m b.s.. Sandy grains are mainly quartz, feldspar and lithic fragments (>30 % of which volcanic) whereas the carbonate fragments are scarce and around 10 % (Fig. 7b). No sediments belonging to this petrofacies have been found in the PM1 core.

Petrofacies B is clustered towards the center of the biplot. Although the spectrum of lithic fragments contained in this petrofacies is similar to that of petrofacies A, petrofacies B contains more carbonate clasts (Fig. 7c), generally above 35%, and sedimentary lithic fragments (Fig. 7d). Micritic limestone fragments are particularly common. Petrofacies B in RB1 core starts above the 27.5 m b.s. peat with the sample RB1-27 (Fig. 6). All samples from PM1 core belong to petrofacies B.

The outlier sample was ascribed to petrofacies C. This shows a composition towards carbonate (>60 % of the total amount) and cherts (10 %), which are normally embedded in the micritic limestones as nodules (Barbieri and Grandesso, 2007); on the other hand, this sample has the lowest amount of quartz (10 %) and all the other parameters, which are below 10 %.

The results compared with the present-day sands of the Brenta, Cismon and Piave rivers (Garzanti et al., 2006; Monegato et al., 2010) show that petrofacies A (RB1-29 and 30) is shifted towards the felsic volcanic component. No modern river shows such a petrofacies. On the other hand, petrofacies B has a good match with the modern Brenta River, which includes the Cismon catchment. Ternary diagrams show a slight shift of petrofacies B towards carbonate components (Fig. 7).

Using the mixing technique after Vezzoli and Garzanti (2009), petrofacies A confirms to be the most similar to the Brenta River sediments upstream the junction with the Cismon River. Petrofacies B is quite similar to the present Brenta River, with an enrichment of carbonate rock fragments that suggests the contribution of a catchment rich in these components. This input could be from the Piave drainage basin, whereas an input from the Astico-Bacchiglione system in the lowlands can be discarded because during the LGM the river was pushed to the west by the development of the Brenta megafan (Rossato et al., 2013; Fontana et al., 2014), which also managed to dam the Lake Fimon south of Vicenza (Monegato et al., 2011). Finally, petrofacies

C shows high values in carbonate and chert parameters (Tab. 2) with no clustering with endmembers (Fig. 7); the mixing technique rules out any possible scenario involving modern endmembers (R^2<0.7; Tab. 2). Petrofacies C belongs to the filling of a post-glacial incision of the Brenta megafan (Mozzi et al., 2013), when only Brenta and Cismon catchments were contributing. Most of the carbonate clasts are micritic limestones that, coupled with the abundance of cherts, suggest an erosion event/phase in the lower Cismon (Corlo) valley north of Rocca (Fig. 1, 3) or in the upper Cismon valley close to Lamon, where these rocks are dominant (Tessari, 1973).

4.5 Mineralogy and geochemistry

Mineralogical analyses of the bulk sediments related to the petrofacies of the cores are reported in terms of main minerals, such as phyllosilicates (mainly micas and chlorites), dolomites (two different crystal chemical terms) and feldspars (plagioclase and k-feldspar), as shown in Fig. 8a. The complete dataset, including mineralogical and geochemical data, is reported in the supplementary material (STab. 1).

Basal sediments in RB1 core (i.e., three deepest samples and a peat sample) are characterized by an enrichment in feldspars and correspond to petrofacies A. The overhead sediments, below the main erosional surface along the core, are characterized by abundance of phyllosilicates, whereas dolomites are depleted; their stratigraphic position corresponds to petrofacies B. Two topmost samples (above the erosional surface), are distinctive for their higher dolomite content and correspond to petrofacies C.

Samples from PM1 core mainly plot as those recognized for petrofacies B in RB1 core, without significant stratigraphic differences along the PM1 core. Although calcite is one of the main minerals observed in the cores, it is not considered as a discriminating variable because it is strongly depleted or even absent in peat sediments (i.e., > 12 wt % organic matter), making this mineral mainly influenced by the depositional environment and, therefore, poorly indicative of the sediment provenance.

The distinctive mineralogical features of samples corresponding to petrofacies A, B and C are also evidenced by sediment chemistry, as reported in Fig. 8b in terms of MgO, Na_2O and Fe_2O_3, because of their affinity for dolomite, plagioclases and fine-grained minerals (clay minerals, oxides and hydroxides). In this case, petrofacies A, B and C are even more clearly discriminated for both cores.

A more detailed evaluation of the bulk mineralogical composition along the RB1 core enables to highlight that both samples corresponding to petrofacies A, B and C are characterized by a peculiar feldspar/quartz ratio (SFig. 1) and that the transition between each group is rather sharp. On the contrary, the feldspar/quartz ratio throughout the PM1 core does not show abrupt variations.

5 Discussion

Data gathered in the mountain area and in the piedmont megafan are here discussed in order to reconstruct the evolution of the LGM Brenta glacier and tributary glacial systems.

5.1 Glaciers in the mountain area

While all the major LGM valley glaciers of the south-eastern Alps preserved all or parts of their end-moraine systems in the terminal valley tracts and/or in the piedmont plain (Venzo et al., 1977; Monegato et al., 2007; Carton et al., 2009; Rossato et al., 2013), in the Brenta valley there is no evidence of the LGM (nor older) terminal moraines (Castiglioni, 2004). The Brenta glacier that used to flow through the Valsugana during the LGM was mainly fed by the Adige glacier, the largest on the southern side of the Alps (Bassetti and Borsato, 2005; Monegato et al., 2017) and some local tributary glaciers from the eastern valley side. The transfluence of Adige glacier into the Valsugana was through the Fersina saddle (550 m a.s.l.) and the Vigolo Vattaro windgap (lowermost altitude: 680 m a.s.l.); more significantly, above the Calisio plateau (ca 1000 m a.s.l.) during the maximum glacier expansion. Flowing for about 50 km along the Valsugana, the glacier reached the Primolano sector where the Valsugana narrows from about 1 km to 100 m and the Canal La Menor windgap opens eastwards at about 350 m a.s.l. (Fig. 2).

Based on the location of marginal glacial deposits, the sudden narrowing of the Brenta valley may have caused the glacier front stabilization, as happened in the northwestern Himalaya during the Late Pleistocene, when narrow steep-walled canyons constituted an effective barrier to glaciers advance (Burbank and Fort, 1985). The subsequent growth of the glacier forced it to rise up to the Canal La Menor windgap and, thus, to split in two lobes (Fig. 2). The eastern lobe flowing across the windgap formed the Sorist (760 to 650 m a.s.l.), Novegno (720 to 600 m a.s.l.) and Guarda (700 to 660 m a.s.l.) lateral moraines; the western lobe built the Enego and Col del Gallo (both ~780 m a.s.l.) lateral moraines. The abundance of porphyry clasts and boulders in the deposits related to both eastern and western lobes indicates sediment provenance from the upper Valsugana and the Adige valley. The differences in elevation of the various moraines suggest that the western lobe grew more than the eastern one, possibly bulging due to the narrowing of the Valsugana. A secondary effect of the glacier bulging would have been the formation of transverse crevasses, producing the fall of supraglacial debris into the ice mass, both hindering the transport of sediments to the glacier front and increasing the hydraulic conductivity of the otherwise effectively impermeable glacier ice (Gulley and Benn, 2007). At the end of the gorge the Valsugana valley widens again, a morphology that likely induced the formation of splaying/radial crevasses and icefalls in the frontal glacier mass (Nye, 1952; Harper et al., 1998; Colgan et al., 2016).

The large stratigraphic section in the Coste quarry, and the minor Valstagna one, displays no evidence of glacial deposits while theyit indicates the presence of important LGM glaciofluvial aggradation in front of the western glacier's fronts. Henceforth, the front of the Brenta glacier flowing in the main valley (western lobe) should have been located between the southernmost end of the Enego and Col del Gallo moraines and the Coste quarry. Glacier confined in narrow valleys normally experience rapid advances under positive mass balance condition: the narrower the valley, the faster the glacier's speed (e.g., Egholm et al., 2011). However, it has been proved that during Late Pleistocene valleys narrowing promoted glaciers blockage in the Himalaya (Burbank and Fort, 1985). This latter is probably the case of this Brenta tongue, the Coste section being only about 250 m downstream of the Enego moraine. The presence of the high-elevation lateral moraines hanging above the valley (the

Enego moraine is about 550 m higher than the present valley floor) at such a short distance from proglacial sediments suggest that when the glacier was at its maximum size its front probably consisted of an icefall. This tongue of the Brenta glacier, being a debris-free glacier, has been characterized by a more effective ablation due to solar energy compared to glaciers covered by several centimeters or more of debris (Lardeux et al., 2015; Wei et al., 2010). The resulting abundant meltwaters fed a well-developed proglacial stream, inducing aggradation along the whole Brenta valley, as testified by the Coste and Valstagna sections. The development of a subglacial/englacial drainage system related to debris-filled crevasses probably controlled the seasonal variation of the glacier, thus resulting in less fluctuations at the glacier's front (van der Veen, 2007). Such stability would result in the growing of the Enego and Col del Gallo lateral moraines. This Brenta glacier tongue may have brought debris at its front both during stability, through supra- and/or englacial transport (Barr and Lovell, 2014 and reference therein), and while advancing, bulldozing preexisting valley-floor sediments (e.g., Winkler and Matthews, 2010). Such debris may have formed end moraines, later eroded by post-glacial fluvial and slope processes. However, considering the narrow gorge that hosted the glacier front, it seems more probable that high-discharge proglacial streams were occupying the entire gorge, continuously removing the incoming debris and precluding the formation of terminal moraines.

When the Brenta glacier reached the elevation of the Canal La Menor windgap, the eastern path became an effective glacial flux, as it happens when stabilized valley glaciers can extend laterally (Barr and Lovell, 2014). The higher the glacier, the more effective would have been the glacial flux through the eastern path, overtopping also the western side of the Novegno plateau. As glacial sediment transport is likely to follow the main glacial flux, the eastern flow probably subtracted increasingly higher portions of the glacially-transported debris to the western one, depleting the sedimentary flux through the Valsugana gorge and further hindering the formation of an end moraine at the western front. The eastern glacial lobe flowed along the Canal La Menor windgap down to the confluence with the Corlo valley. Here, it merged with the glacier coming from the north-east, formed by the contribution of both the Cismon glacier and the westernmost lobe of the Piave glacier, as testified by the Roncon till. This latter deposit is polygenic, with pebbles of dolostones and Triassic volcanic rocks belonging to the Piave catchment. This latter till crops out extensively also in the nearby Seren valley, into which a lateral tongue of the Piave glacier was flowing. Geomorphic evidence of the westward flow of Piave glacier is provided by the lateral moraines at Monache (750 to 650 m a.s.l.), even though they are made mostly of limestone clasts, thus reflecting a local glacigenic sedimentary input.

The glacier deriving from the merging of the eastern Brenta lobe and the Cismon/Piave glaciers, at the confluence of Canal La Menor and the Corlo valley, left no traces of frontal moraines. Glacial till crops out close to Rocca (Fig. 2) and till patches were described about 0.5 km southwards (Dal Piaz et al., 1946), suggesting that the front of this glacier was located at the beginning of the narrow gorge now occupied by the southern end of the artificial Lake Corlo. The geomorphological setting is very similar to the western tongue, suggesting that also here the glacier's front may have consisted in an icefall with deep crevasses without terminal moraines.

The Valsugana glacier left a remarkably small amount of erratics. During our survey, a total amount of 7 boulders made of porphyry and granite, up to 1 m large, have been found (Novegno and Sorist areas). Other authors mentioned erratics on top

of the Novegno plateau (up to 2 m large and made of crystalline rocks), next to the Enego moraine ("very large" boulders made of carbonate rocks; Secco, 1883; Venzo, 1940) and on the Canal La Menor valley bottom ("extremely large" porphyry boulders; Taramelli, 1882). No erratics have been found, nor mentioned, downstream along the Valsugana valley bottom.

5.2 The fluvial record of glaciers' changes

The fluvial sediments cropping out in the Coste and Valstagna quarries are the only remnants of the LGM glaciofluvial aggradation that took place downstream of both eastern and western glaciers' fronts. This glaciofluvial sedimentation led to the infilling of the Valsugana valley bottom up to some tens of meters above the present Brenta river. The elevation of the top of the LGM valley fill at Coste (about 225 m a.s.l.) is consistent with the one of the Valstagna section (about 175 m a.s.l.) as well as with the top LGM surface of the Brenta megafan SE of Bassano del Grappa (about 130 m a.s.l.). This allows the correlation of these depositional top surfaces and the related sediments, as well as the reconstruction of the longitudinal profile of the LGM Brenta valley bottom (Fig. 9). The LGM fluvial aggradation was followed by the incision of the valley bottom and the piedmont megafan at around 17.5 ka cal BP, as the fluvial system reacted to the downwasting of the glacial system (Mozzi, 2005; Fontana et al., 2014; Rossato and Mozzi, 2016).

The growth/collapse of glacial tongues and modifications in the fluvial networks can be detected from changes in the mountain catchments and in the alluvial plain. Sedimentary systems developing at the mouth of major valleys are highly valuable databases of sedimentary, climatic and tectonic data (e.g., Mozzi et al., 2005; Carton et al., 2009; Pini et al., 2009; Piovan et al., 2012; Rossato and Mozzi, 2016). The paucity of radiocarbon datable material usually available in glacial deposits can be balanced with the abundant organic samples that can be collected in fluvial sedimentary sequences of this area. In our investigation, the petrographic, mineralogical and geochemical and analyses of RB1 and PM1 cores in the glaciofluvially-fed Brenta megafan, chronologically framed through radiocarbon dating, integrate the evidence obtained in the mountain area. This allowed to distinguish specific evolutionary phases in the drainage network feeding the Brenta megafan (Fig. 10), described as follows from the oldest one:

- The first phase, testified in the RB1 core, corresponds to petrofacies A and lasted up to straight after 27 ka cal BP. At that time glaciers were growing at the onset of LGM (Monegato et al., 2007; 2017; Ivy-Ochs et al., 2008; Preusser et al., 2011) and the mountain drainage systems began to modify. The Brenta megafan sedimentation rates were still comparable to pre-LGM ones (Rossato and Mozzi, 2016). Sediments indicate that this megafan was fed by a river with a drainage system limited to the Valsugana, as shown by the petrographic samples (RB1-29 and 30). The Cismon drainage system, which is currently merging with the Brenta one, was not contributing, as it was probably flowing eastwards into the Piave one (Fig. 10).
- The beginning of the second phase coincided to a gradually increasing change in the drainage system, as testified by mineralogical and petrographic analyses of petrofacies B (samples RB1-27, 24, 21 and 16 and PM1-19, 17 and 12) (Figs. 7-8). Radiocarbon dates indicate that this phase started straight after 27 ka cal BP and continued after 20.1 ka cal BP (Fig. 6). The lack of major unconformities in the succession of PM1 core suggests that the top of this phase

corresponds to the LGM surface of the Brenta megafan, implying that sedimentation lasted until 17.5 ka cal BP (Rossato and Mozzi, 2016). Soon after 27 ka cal BP, the Piave and Cismon systems began to contribute to the Brenta one through the Corlo valley. Whilst the Cismon river diversion do not require a direct connection with glacier dynamics, the Piave glacier must have grown enough to overcome the Seren saddle (~330 m a.s.l.; Figs. 1, 10), about 100 m above the current Piave valley bottom. At the acme of LGM, the contribution of these systems is likely to have blown up the sedimentation rates in the Brenta megafan, that nearly doubled in the 26.7-23.8 ka cal BP period (Rossato and Mozzi, 2016; Fig. 10). The Piave glacier tongue overcoming the Seren saddle probably survived the ~19.5 ka cal BP glacial retreat, as the main glacier was still being 500 m thick near Belluno ("Val Piana" stage: 16.210 ± 50 years BP, Pellegrini et al., 2005, recalibrated to 19,386 - 19,772 years cal BP with IntCal13 calibration curve, Reimer et al., 2013).

- The youngest phase is recorded only in the topmost sediments of RB1 core, constituting petrofacies C. It is ascribable to the infilling of a fluvial entrenchment (Fig. 2) developed during late stages of deglaciation (Mozzi et al., 2013), as occurred elsewhere in the whole Central and Eastern Po Plain (Fontana et al., 2014). Mineralogy confirms the present configuration of the drainage system, with the Cismon River flowing into the Brenta River through the Corlo valley and the Piave River already flowing along its modern valley. However, a remarkable enrichment in carbonates (micritic limestones) in respect to modern Brenta sediments, testified by petrography, mineralogy and geochemistry, highlights an anomalous setting. Two possible scenarios may be proposed to explain such signal: i) a significant bedrock erosion of these lithologies in the mountain area (i.e. especially in the Cismon catchment), or ii) a connection with the dismantling of the postulated landslide that induced the aggradation of the Lamon terraces (if the "landslide scenario" is assumed; see the Setting chapter for details). The first hypothesis can relate to the carving of the Corlo valley by Cismon River during the Lateglacial when high meltwater discharges could easily induce such enhanced erosion stages, as normally occurs during glacier recessional phases (Herman et al., 2011).

6 Conclusions

The acquired dataset casts new light on the dynamics of the LGM glaciers in the canyon-like, middle tract of a major Alpine valley, the Valsugana. The knot of the Valsugana glacier has been disentangled for the first time, indicating a singular configuration of the glacier snouts crossing narrow and deep valley reaches.

Our data indicates that at the LGM acme the Brenta glacier split at Primolano. One tongue used to flow southwards along the Valsugana valley through a narrow gorge which prevented an effective glacier flux and caused the glacier's bulging. The bulging forced the right side of the glacial tongue to reach high elevation at Enego, while its front was probably constituted by an icefall located just upstream of Coste. Meltwaters were flowing in subglacial and englacial streams removing debris from the glacier front and filling the Valsugana valley bottom. The other tongue collected most of the glacial and debris fluxes, flowing eastwards along the Canal La Menor valley and joining the Cismon/Piave glacier near Rocca.

The coupling of data gathered in the mountain area with those collected in the piedmont alluvial plain allows a coherent reconstruction of the dynamics of the LGM glacier tongues. Prior to the arrival of the glacier fronts in the study area, the Brenta megafan received sediments only from the upper Valsugana catchment. A major alteration of the drainage system occurred just before 27 ka cal BP, when the Cismon and Piave systems joined the Brenta River in the Valsugana valley, through the Seren saddle and the Corlo valley. Between ~27 and, at least, ~19.5 ka cal BP, the Brenta, Cismon and Piave glaciers were merging in the surroundings of the Novegno mount. Their meltwaters were building up the largest alluvial landform of the whole Po Plain at that time: the Brenta megafan. At the end of the LGM, the waning of glaciers induced the fluvial incision of the Brenta megafan. The abundance of micritic carbonates in the sedimentary fill of such incisions near Piazzola sul Brenta suggests a concomitant remarkable bedrock erosion in the Corlo valley and/or the reworking of sediments from the Cismon catchment at Lamon.

As general conclusive remarks, this study highlights that:

- the narrowing of a main glaciated valley may result in the blockage/slowing of the glacier flux. A larger lateral valley may easily represent an alternative path for the glacier, even if its bottom lies at higher elevation, subtracting large part of the glacial and debris flux from the main valley;
- valley glaciers flowing across narrow gorges may be subject to bulging and likely have icefalls at their front, while proglacial meltwater streams prevent the formation of end moraines;
- in rugged Alpine terrains, glacial catchments may significantly vary over time during a single glaciation. Such changes affect both the glacial and glaciofluvial systems and can be recognized in the alluvial stratigraphic record far downstream from the glacier front. Sand petrography and chemical/mineralogical composition of sediments are good tracers of glacial catchment variations.

Acknowledgements

We sincerely thank S. Winkler and L. Stutenbecker for thorough critical reviews that greatly improved the quality of the manuscript.

Author contributions

All authors contributed to interpreting results and improving the text, that has been written mostly by S. Rossato. Each author contributed to different parts, here listed: field survey: S. Rossato, G. Monegato, P. Mozzi; sand petrography: G. Monegato; X-ray diffraction: A. Carraro, F. Tateo; chemical composition: A. Carraro, F. Tateo; core description: S. Rossato, P. Mozzi; remote sensing: S. Rossato.

Competing interests

The authors declare that they have no conflict of interest.

References

ARPAV: Carta dei suoli del Veneto in scala 1: 250.000. Grafiche Vianello, Treviso, 2005.

Aitchinson, J. And Greenacre, M.: Biplots of compositional data, J. Roy. Stat. Soc. C-App., 51(4), 375-392, doi: 10.1111/1467-9876.00275, 2002.

Avanzini, M., Bargossi, G. M., Borsato, A. and Selli, L.: Note Illustrative della Carta Geologica d'Italia alla scala 1: 50.000, foglio 060- Trento, ISPRA-Servizio Geologico d'Italia, Trento, 2010.

Baratto, A., Ferrarese, F., Meneghel, M. and Sauro, U.: La ricostruzione della glaciazione wurmiana nel Gruppo del Monte Grappa (Prealpi Venete), in: Biancotti, A. and Motta, M. (eds.): Risposta dei processi geomorfologici alle variazioni ambientali, Brigati G., Genova, Italy, 67-77, 2003.

Barbieri, G. and Grandesso, P.: Note illustrative della Carta Geologica d'Italia alla scala 1: 50.000, foglio 082-Asiago, APAT, S.EL.CA., Firenze, 135, 2007.

Barr, I. D. and Lovell, H.: A review of topographic controls on moraine distribution, Geomorphology, 226, 44-64, doi: 10.1016/j.geomorph.2014.07.030, 2014.

Bartolomei, G., Corsi, M., Dal Cin, R., D'Amico, C., Gatto, G. O., Gatto, P., Nardin, M., Rossi, D., Sacerdoti, M. and Semenza, E.: Note illustrative della carta geologica d'Italia alla scala 1: 100.000, foglio 021-Trento, Poligrafica e Cartevalori, Ercolano, 1969

Bartolomei, G.: Nuovi elementi su un morenico antico a Bassano del Grappa, Vicenza, in: Orombelli, G. (ed.): Studi geografici e geologici in onore di Severino Belloni, 9-18, 1999.

Bassetti, M. and Borsato, A.: Evoluzione geomorfologica della Bassa Valle dell'Adige dall'Ultimo Massimo Glaciale: sintesi delle conoscenze e riferimenti ad aree limitrofe, Studi Trent. Sci. Nat.-Acta Geol., 82, 31-42, 2005.

Becker, P., Seguinot, J., Jouvet, G. and Funk, M.: Last Glacial Maximum precipitation pattern in the Alps inferred from glacier modelling, Geogr. Helv., 71(3), 173-187, doi: 10.5194/gh-71-173-2016, 2016.

Bigi, G., Castellarin, A., Coli, M., Dal Piaz, G. V., Sartori, R., Scandone, P. and Vai, G. B.: Structural Model of Italy, sheets 1, CNR, S.EL.CA., Firenze, 1990.

Bowen, D. Q.: Last glacial maximum, in: Encyclopedia of Paleoclimatology and Ancient Environments (pp. 493-495). Springer Netherlands, 2009.

Brauer, A., Hajdas, I., Blockley, S. P., Ramsey, C. B., Christl, M., Ivy-Ochs, S., Moseley, G. E., Nowaczyk, N. N., Rasmussen, S. O., Roberts, H. M., Spötl, C., Staff, R. A. and Svensson, A.: The importance of independent chronology in integrating records of past climate change for the 60-8 ka INTIMATE time interval, Quaternary Sci. Rev., 106, 47-66, doi: 10.1016/j.quascirev.2014.07.006, 2014.

Buccianti, A., Pawlowsky-Glahn, V., Barceló-Vidal, C. and Jarauta-Bragulat, E.: Visualization and modeling of natural trends in ternary diagrams: a geochemical case study, in Lippard, S. J., Naess, A. and Sinding-Larsen, R. (eds.): Proceedings of IAMG'99 - The fifth annual conference of the International Association for Mathematical Geology: Trondheim, 139-144, 1999.

Burbank, D. W. and Fort, M. B.: Bedrock control on glacial limits: examples from the Ladakh and Zanskar ranges, north-western Himalaya, India, J. Glaciol., 31(108), 143-149, 1985.

Carraro, A., Fabbri, P., Giaretta, A., Peruzzo, L., Tateo, F. and Tellini, F.: Arsenic anomalies in shallow Venetian Plain (Northeast Italy) groundwater, Environ. Earth Sci., 70(7), 3067-3084, doi: 10.1007/s12665-013-2367-2, 2013.

Carraro, A., Fabbri, P., Giaretta, A., Peruzzo, L., Tateo, F. and Tellini, F.: Effects of redox conditions on the control of arsenic mobility in shallow alluvial aquifers on the Venetian Plain (Italy), Sci. Total Environ., 532, 581-594, doi: 10.1016/j.scitotenv.2015.06.003, 2015.

Carraro, F. and Sauro, U.: Il Glacialismo "locale" Wurmiano del Massiccio del Grappa (Provincie di Treviso e di Vicenza), Geogr. Fis. Dinam. Quat., 2(1), 6-16, 1979.

Carraro, F., Grandesso, P., Sauro, U. and Paoletti, G.: Incontri con il Grappa: i segreti della geologia, Moro Edizioni, 1989.

Carton, A., Bondesan, A., Fontana, A., Meneghel, M., Miola, A., Mozzi, P., Primon, S. and Surian, N.: Geomorphological evolution and sediment transfer in the Piave River system (northeastern Italy) since the Last Glacial Maximum, Géomorphologie, 15(3), 155-174, doi: 10.4000/geomorphologie.7639, 2009.

Castellarin, A., Nicolich, R., Fantoni, R., Cantelli, L., Sella, M. and Selli, L.: Structure of the lithosphere beneath the Eastern Alps (southern sector of the TRANSALP transect), Tectonophysics, 414(1-4), 259-282, doi: 10.1016/j.tecto.2005.10.013, 2006.

Castiglioni, B.: L'Italia nell'età quaternaria. Atlante Fisico-economico d'Italia, Consociazione Turistica Italiana, Milano, Italy, 1940.

Castiglioni, G. B.: Quaternary glaciations in the eastern sector of the Italian Alps, in: Elhers, J. and Gibbard, P. (eds): Quaternary Glaciations-Extent and Chronology, 209-215, doi: 10.1016/S1571-0866(04)80072-1, 2004.

Castiglioni, G. B., Meneghel, M. and Sauro, U.: Elementi per una ricostruzione dell'evoluzione morfotettonica delle Prealpi Venete, Geogr. Fis. Dinam. Quat. suppl, 1(1988), 31-44, 1988.

Clark, P. U., Dyke, A. S., Shakun, J. D., Carlson, A. E., Clark, J., Wohlfarth, B., Mitrovica, J. X., Hostetler, S. W. and McCabe, A. M.: The last glacial maximum, Science, 325(5941), 710-714, doi: 10.1126/science.1172873, 2009.

Colgan, W., Rajaram, H., Abdalati, W., McCutchan, C., Mottram, R., Moussavi, M. S. and Grigsby, S.: Glacier crevasses: Observations, models and mass balance implications, Rev. Geophys., 54(1), 119-161, doi: 10.1002/2015RG000504, 2016.

Comas, M., Thió- Henestrosa, S.: CoDaPack 2.0: a stand-alone multi-platform compositional software, in: Egozcue, J.J., Tolosana-Delgado, R. and Ortego, M.I. (Eds.), CoDaWork'11: 4th International Workshop on Compositional Data Analysis. Saint Feliu de Guixols, Girona, Spain, 2011.

Cucato, M.: Rilevamento della media Val d'Astico (Provincia di Vicenza): saggio per l 'applicazione della normativa sulla cartografia geologica del Quaternario continentale, B. Serv. Geol. Ital., 99-130, 2001.

Dal Piaz, G., Fabiani, R., Trevisan, L., Venzo, S.: Carta geologica delle tre Venezie al 100.000, foglio 37-Bassano del Grappa, Ufficio Idrografico Magistrato delle Acque, Venezia, 1946.

Egholm, D. L., Knudsen, M. F., Clark, C. D., Lesemann, J. E.: Modeling the flow of glaciers in steep terrains: The integrated second-order shallow ice approximation (iSOSIA), J. Geophys. Res.-Earth, 116 (F02012), doi: 10.1029/2010JF001900, 2011.

Evans, I. S.: Glacier distribution in the Alps: statistical modelling of altitude and aspect, Geogr. Ann. A, 88(2), 115-133, doi: 10.1111/j.0435-3676.2006.00289.x, 2006.

Fao, I. ISSS: World reference base for soil resources, 84, 1998.

Florineth, D. and Schlüchter, C.: Alpine evidence for atmospheric circulation patterns in Europe during the Last Glacial Maximum, Quaternary Res., 54(3), 295-308, doi: 10.1006/qres.2000.2169, 2000.

Fontana, A., Mozzi, P. and Bondesan, A.: Alluvial megafans in the Venetian-Friulian Plain (north-eastern Italy): Evidence of sedimentary and erosive phases during Late Pleistocene and Holocene, Quaternary Int., 189(7), doi: 10.1016/j.quaint.2007.08.044, 2008.

Fontana, A., Monegato, G., Zavagno, E., Devoto, S., Burla, I. and Cucchi, F.: Evolution of an Alpine fluvioglacial system at the LGM decay: the Cormor megafan (NE Italy), Geomorphology, 204, 136-153, doi: 10.1016/j.geomorph.2013.07.034, 2014.

Garzanti, E. ando, S. and Vezzoli, G.: The continental crust as a source of sand (southern Alps cross section, northern Italy), J. Geol., 114(5), 533-554, doi: 10.1086/506159, 2006.

Garzanti, E. Andó, S., France-Lanord, C., Censi, P., Vignola, P., Galy, V. and Lupker, M.: Mineralogical and chemical variability of fluvial sediments 2. Suspended-load silt (Ganga-Brahmaputra, Bangladesh), Earth Planet. Sc. Lett., 302(1-2), 107-120, doi: 10.1016/j.epsl.2010.11.043, 2011.

Gazzi, P., Zuffa, G. G., Gandolfi, G. and Paganelli, L.: Provenienza e dispersione litoranea delle sabbie delle spiagge adriatiche fra le foci dell'Isonzo e del Foglia: inquadramento regionale, Mem. Soc. Geol. Ital., 12(1), 1-37, 1973.

Harper, J. T., Humphrey, N. F. and Pfeffer, W. T.: Crevasse patterns and the strain-rate tensor: a high-resolution comparison, J. Glaciol., 44(146), 68-76, doi: 10.3189/S0022143000002367, 1998.

Heiri, O., Koinig, K. A., Spötl, C., Barrett, S., Brauer, A., Drescher-Schneider, R., Gaar, D., Ivy-Ochs, S., Kerschner, H., Luetscher, M., Moran, A., Nicolussi, K., Preusser, F., Schmidt, R., Schoeneich, P., Schwörer, C., Sprafke, T., Terhorst, B. and Tinner, W.: Palaeoclimate records 60-8 ka in the Austrian and Swiss Alps and their forelands, Quaternary Sci. Rev., 106, 186-205, doi: 10.1016/j.quascirev.2014.05.021, 2014.

Herman, F., Anderson, B. and Leprince, S.: Mountain glacier velocity variation during a retreat/advance cycle quantified using sub-pixel analysis of ASTER images, J. Glaciol., 57(202), 197-207, doi: 10.3189/002214311796405942, 2011.

Hughes, P. D. and Gibbard, P. L.: A stratigraphical basis for the Last Glacial Maximum (LGM), Quaternary Int., 383, 174-185, doi: 10.1016/j.quaint.2014.06.006, 2015.

Ingersoll, R. V., Bullard, T. F., Ford, R. L., Grimm, J. P., Pickle, J. D. and Sares, S. W.: The effect of grain size on detrital modes: a test of the Gazzi-Dickinson point-counting method, J. Sediment. Res., 54(1), 103-116, 1984.

Ivy-Ochs, S.: Glacier variations in the European Alps at the end of the last glaciation, Cuadernos Invest. Geogr., 41(41), 295-315, doi: 10.18172/cig.2750, 2015.

Ivy-Ochs, S., Kerschner, H., Reuther, A., Preusser, F., Heine, K., Maisch, M., Kubik, P. W. and Schlüchter, C.: Chronology of the last glacial cycle in the European Alps, J. Quaternary Sci., 23(6-7), 559-573, doi: 10.1002/jqs.1202, 2008.

Kelly, M. A., Buoncristiani, J. F. and Schlüchter, C.: A reconstruction of the last glacial maximum (LGM) ice-surface geometry in the western Swiss Alps and contiguous Alpine regions in Italy and France, Eclogae Geol. Helv., 97(1), 57-75, doi: 10.1007/s00015-004-1109-6, 2004.

Koppes, M. N. and Montgomery, D. R.: The relative efficacy of fluvial and glacial erosion over modern to orogenic timescales, Nat. Geosci., 2(9), 644, doi: 10.1038/ngeo616, 2009.

Lardeux, P., Glasser, N. F., Holt, T., Irvine-Fynn, T. D. and Hubbard, B. P.: Area and Elevation Changes of a Debris-Covered Glacier and a Clean-Ice Glacier Between 1952-2013 Using Aerial Images and Structure-from-Motion. AGU Fall Meeting Abstracts, doi: 10.13140/RG.2.1.5059.4329, 2015.

Luetscher, M., Boch, R., Sodemann, H., Spötl, C., Cheng, H., Edwards, R. L., Frisia, S., Hof, F. and Müller, W.: North Atlantic storm track changes during the Last Glacial Maximum recorded by Alpine speleothems, Nat. Commun., 6, 6344, doi: 10.1038/ncomms7344, 2015.

Massari, F., Grandesso, P., Stefani, C. and Zanferrari, A.: The Oligo-Miocene Molasse of the Veneto-Friuli region, Southern Alps, Giorn. Geol., 48(1-2), 235-255, 1986.

Miola, A., Bondesan, A., Corain, L., Favaretto, S., Mozzi, P., Piovan, S. and Sostizzo, I.: Wetlands in the Venetian Po Plain (northeastern Italy) during the Last Glacial Maximum: Interplay between vegetation, hydrology and sedimentary environment, Rev. Palaeobot. Palyno., 141(1-2), 53-81, doi: 10.1016/j.revpalbo.2006.03.016, 2006.

Monegato, G., Ravazzi, C., Donegana, M., Pini, R., Calderoni, G. and Wick, L.: Evidence of a two-fold glacial advance during the last glacial maximum in the Tagliamento end moraine system (eastern Alps), Quaternary Res., 68(2), 284-302, doi: 10.1016/j.yqres.2007.07.002, 2007.

Monegato, G., Stefani, C. and Zattin, M.: From present rivers to old terrigenous sediments: the evolution of the drainage system in the eastern Southern Alps, Terra Nova, 22(3), 218-226, doi: 10.1111/j.1365-3121.2010.00937.x, 2010.

Monegato, G., Pini, R., Ravazzi, C., Reimer, P. J. and Wick, L.: Correlating Alpine glaciation with Adriatic sea-level changes through lake and alluvial stratigraphy, J. Quaternary Sci., 26(8), 791-804, doi: 10.1002/jqs.1502, 2011.

Monegato, G., Scardia, G., Hajdas, I., Rizzini, F. and Piccin, A.: The Alpine LGM in the boreal ice-sheets game, Sci. Rep.-UK, 7(1), 2078, doi: 10.1038/s41598-017-02148-7, 2017.

Mozzi, P.: L'alta e media pianura del Brenta, in Bondesan, A., Caniato, G., Gasperini, D., Vallerani F. and Zanetti M. (Eds.): Il Brenta, Cierre Edizioni, Verona, pp. 39-53, 2003.

Mozzi, P.: Alluvial plain formation during the Late Quaternary between the southern Alpine margin and the Lagoon of Venice (northern Italy), Geogr. Fis. Dinam. Quat., 7, 219-230, 2005.

Mozzi, P., Piovan, S., Rossato, S., Cucato, M., Abbà, T. and Fontana, A.: Palaeohydrography and early settlements in Padua (Italy), Il Quaternario-Ital. J. Quaternary Sci., 23, 387-400, 2010.

Mozzi, P., Ferrarese, F. and Fontana, A.: Integrating digital elevation models and stratigraphic data for the reconstruction of the post-LGM unconformity in the Brenta alluvial megafan (North-Eastern Italy), Alp. Mediterr. Quaternary, 26, 41-54, 2013.

Norton, K. P., Abbühl, L. M. and Schlunegger, F.: Glacial conditioning as an erosional driving force in the Central Alps, Geology, 38(7), 655-658, doi: 10.1130/G31102.1, 2010.

Nye, J. F.: The mechanics of glacier flow, J. Glaciol., 2(12), 82-93, doi: 10.3189/S0022143000033967, 1952.

Pellegrini, G. B., Albanese, D., Bertoldi, R. and Surian, N.: La deglaciazione alpina nel Vallone Bellunese, Alpi meridionali orientali, Geogr. Fis. Dinam. Quat. suppl., 7, 271-280, 2005.

Penck, A. and Brückner, E.: Die Alpen im Eiszeitalter, Tauchnitz, Leipzig, 1909.

Piovan, S., Mozzi, P. and Zecchin, M.: The interplay between adjacent Adige and Po alluvial systems and deltas in the late Holocene (Northern Italy), Géomorphologie, 18(4), 427-440, doi: 10.4000/geomorphologie.10034, 2012.

Pini, R., Ravazzi, C. and Donegana, M.: Pollen stratigraphy, vegetation and climate history of the last 215 ka in the Azzano Decimo core (plain of Friuli, north-eastern Italy), Quaternary Sci. Rev., 28(13-14), 1268-1290, doi: 10.1016/j.quascirev.2008.12.017, 2009.

Preusser, F., Reitner, J. M. and Schlüchter, C.: Distribution, geometry, age and origin of overdeepened valleys and basins in the Alps and their foreland, Swiss J. Geosci., 103(3), 407-426, doi: 10.1007/s00015-010-0044-y, 2010.

Preusser, F., Graf, H. R., Keller, O., Krayss, E. and Schlüchter, C.: Quaternary glaciation history of northern Switzerland, E&G-Quaternary Sci. J., 60, 282-305, doi: 10.3285/eg.60.2-3.06, 2011.

Ramsey, C. B.: Bayesian analysis of radiocarbon dates, Radiocarbon, 51(1), 337-360, doi: 10.1017/S0033822200033865, 2009.

Ravazzi, C., Badino, F., Marsetti, D., Patera, G. and Reimer, P. J.: Glacial to paraglacial history and forest recovery in the Oglio glacier system (Italian Alps) between 26 and 15 ka cal BP, Quaternary Sci. Rev., 58, 146-161, doi: 10.1016/j.quascirev.2012.10.017, 2012.

Reimer, P.J., Bard, E., Bayliss, A., Beck, J.W., Blackwell, P.G., Bronk Ramsey, C., Buck, C.E., Cheng, H., Edwards, R.L., Friedrich, M., Grootes, P.M., Guilderson, T.P., Haflidason, H., Hajdas, I., Hatté, C., Heaton, T.J., Hoffmann, D.L., Hogg, A.G., Hughen, K.A., Kaiser, K.F., Kromer, B., Manning, S.W., Niu, M., Reimer, R.W., Richards, D.A., Scott, E.M., Southon, J.R., Staff, R.A., Turney, C.S.M. and van der Plicht, J.: IntCal13 and Marine13 radiocarbon age calibration curves 0-50,000 years cal BP, Radiocarbon, 55(4), 1869-1887, doi: 10.2458/azu_js_rc.55.16947, 2013.

Rossato, S., Monegato, G., Mozzi, P., Cucato, M., Gaudioso, B. and Miola, A.: Late Quaternary glaciations and connections to the piedmont plain in the prealpine environment: the middle and lower Astico Valley (NE Italy), Quaternary Int., 288, 8-24, doi: 10.1016/j.quaint.2012.03.005, 2013.

Rossato, S. and Mozzi, P.: Inferring LGM sedimentary and climatic changes in the southern Eastern Alps foreland through the analysis of a 14C ages database (Brenta megafan, Italy), Quaternary Sci. Rev., 148, 115-127, doi: 10.1016/j.quascirev.2016.07.013, 2016.

Russell, A. J., Roberts, M. J., Fay, H., Marren, P. M., Cassidy, N. J., Tweed, F. S. and Harris, T.: Icelandic jökulhlaup impacts: implications for ice-sheet hydrology, sediment transfer and geomorphology, Geomorphology, 75(1-2), 33-64, doi: 10.1016/j.geomorph.2005.05.018, 2006.

Sacco, F.: Il Glacialismo veneto, L'Universo, 7, 1-40, 1937.

Samartin, S., Heiri, O., Kaltenrieder, P., Kühl, N. and Tinner, W.: Reconstruction of full glacial environments and summer temperatures from Lago della Costa, a refugial site in Northern Italy, Quaternary Sci. Rev., 143, 107-119, doi: 10.1016/j.quascirev.2016.04.005, 2016.

Schlüchter, C.: The Quaternary glaciations of Switzerland, with special reference to the Northern Alpine Foreland, Quaternary Sci. Rev., 5, 413-419, doi: 10.1016/0277-3791(86)90206-4, 1986.

Secco, A.: Note geologiche sul Bassanese. Stabilimento Tipografico Sante Pozzato, 1883.

Seguinot, J., Jouvet, G., Huss, M., Funk, M. and Preusser, F.: Modelling last glacial cycle ice dynamics in the Alps, EGU Abstracts, 19, 8982, 2017.

Smiatek, G., Kunstmann, H., Knoche, R. and Marx, A.: Precipitation and temperature statistics in high-resolution regional climate models: Evaluation for the European Alps, J. Geophys. Res.-Atmos., 114(D19), 2009.

Stefani, C., Fellin, M. G., Zattin, M., Zuffa, G. G., Dalmonte, C., Mancin, N. and Zanferrari, A.: Provenance and paleogeographic evolution in a multi-source foreland: the Cenozoic Venetian-Friulian Basin (NE Italy), J. Sediment. Res., 77(11), 867-887, doi: 10.2110/jsr.2007.083, 2007.

Taramelli, T.: Geologia delle provincie venete. Atti della reale Accademia dei Lincei, 8, 303-541, 1882.

Tessari, F.: Geomorfologia del bacino di Lamon, Val Cismon, Alpi Dolomitiche, Museo Tridentino di Scienze Naturali, 1973.

Torma, C., Giorgi, F. and Coppola, E.: Added value of regional climate modeling over areas characterized by complex terrain—Precipitation over the Alps, J. Geophys. Res.-Atmos., 120(9), 3957-3972, doi: 10.1002/2014JD022781, 2015.

Trevisan, L.: Il glacialismo quaternario nell'Altipiano dei Sette Comuni (Vicenza), Stabilimento tipografico Villarboito F. e figli, 1939.

van der Veen, C. J.: Fracture propagation as means of rapidly transferring surface meltwater to the base of glaciers, Geophys. Res. Lett., 34(1), doi: 10.1029/2006GL028385, 2007.

van Husen, D.: Die Ostalpen in den Eiszeiten, Geol. Bundes., 1987.

van Husen, D. and Reitner, J. M.: An outline of the Quaternary stratigraphy of Austria, E&G-Quaternary Sci. J., 60, 366-387, doi: 10.3285/eg.60.2-3.09, 2011.

Venzo, S.: Studio geotettonico del Trentino meridionale-orientale tra Borgo Valsugana e il Monte Coppolo, Poligrafico dello Stato, Roma, pp. 86, 1940.

Venzo, S.: I depositi quaternari e del neogene superiore nella bassa valle del Piave da Quero al Montello e del Paleopiave nella valle del Soligo (Treviso), Memorie degli Istituti Mineralogia e Geologia dell'Università di Padova, 30, 1-64, 1977.

Vezzoli, G. and Garzanti, E.: Tracking paleodrainage in Pleistocene foreland basins, J. Geol., 117(4), 445-454, doi: 10.1086/598946, 2009.

von Eynatten, H., Pawlowsky-Glahn, V. and Egozcue, J. J.: Understanding perturbation on the simplex: A simple method to better visualize and interpret compositional data in ternary diagrams. Math. Geol., 34(3), 249-257, 2002.

Wei, Y., Tandong, Y., Baiqing, X. and Hang, Z.: Influence of supraglacial debris on summer ablation and mass balance in the 24K Glacier, southeast Tibetan Plateau, Geogr. Ann. A, 92(3), 353-360, doi: 10.1111/j.1468-0459.2010.00400.x, 2010.

Winkler, S., Matthews, J. A.: Observations on terminal moraine-ridge formation during recent advances of southern Norwegian glaciers, Geomorphology, 116, 87-106, doi: 10.1016/j.geomorph.2009.10.011, 2010.

Wirsig, C., Zasadni, J., Christl, M., Akçar, N. and Ivy-Ochs, S.: Dating the onset of LGM ice surface lowering in the High Alps, Quaternary Sci. Rev., 143, 37-50, doi: 10.1016/j.quascirev.2016.05.001, 2016.

Young, R. A.: The Rietveld method, Oxford University Press, pp. 298, 1993.

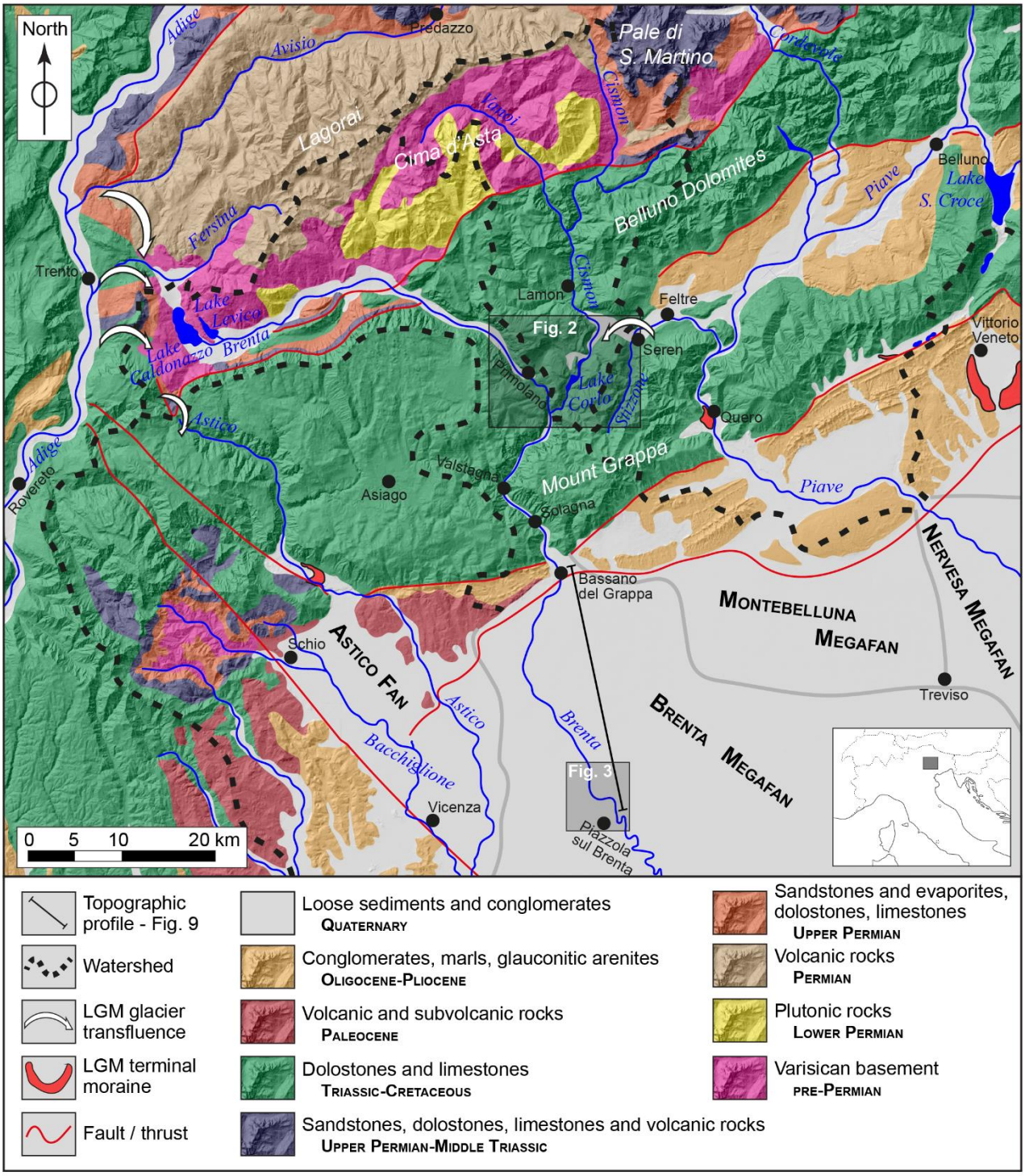

Figure 1: Geological sketch of the study area. The map is based on the Structural Model of Italy (Bigi et al., 1990) and local geological maps (Bartolomei et al., 1969; Dal Piaz et al., 1946; Barbieri and Grandesso, 2007; Avanzini et al., 2010) and it overlies a SRTM-derived Digital Elevation Model (30-m large cells) [source: http://viewfinderpanoramas.org/].

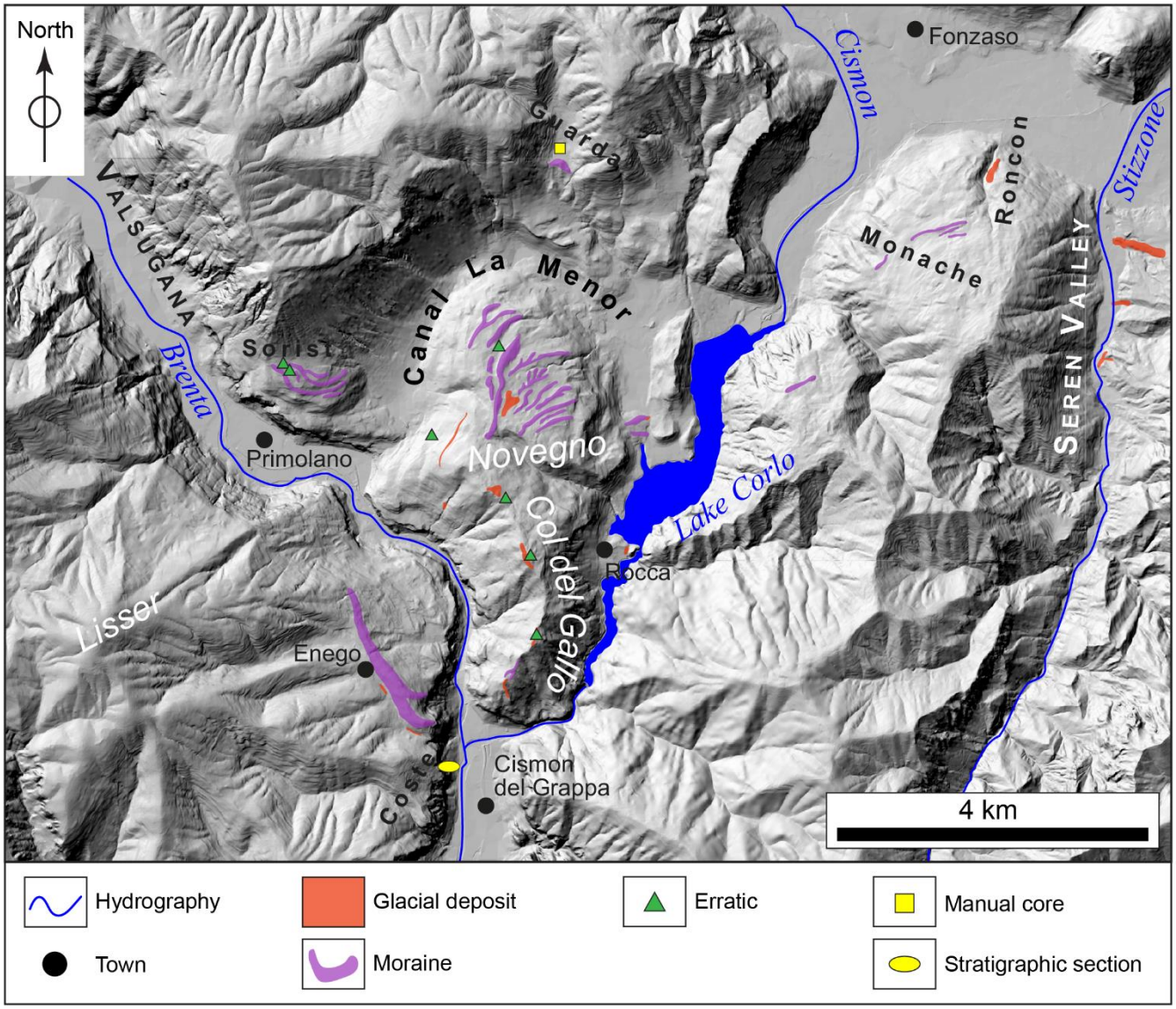

Figure 2: Outcrops map of the middle Valsugana sector derived from field surveys and remote sensing data. Polygons/symbols overlie a 5-m cell DTM (modified from data provided by Regione Veneto, 2011).

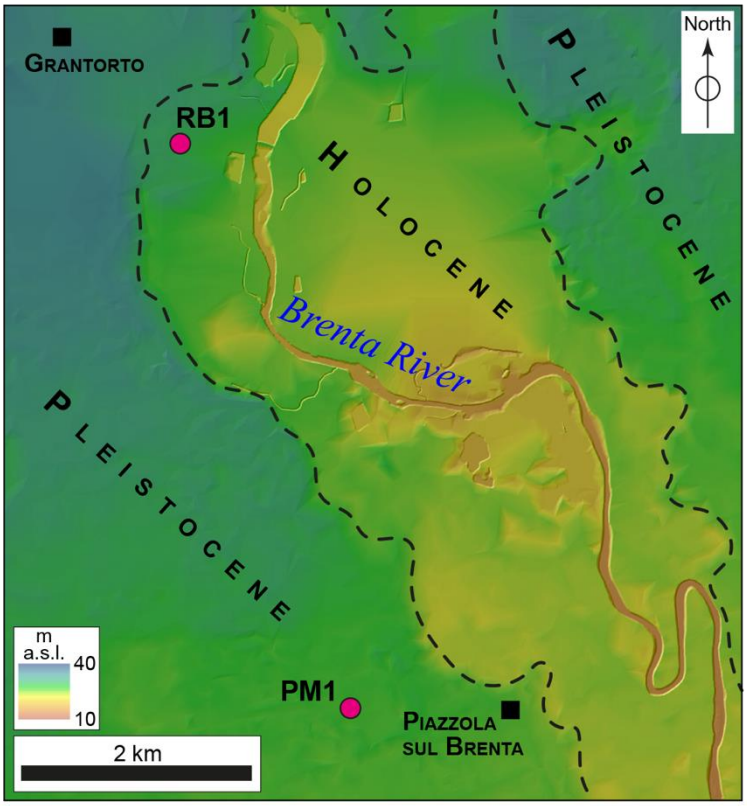

Figure 3: Location of the PM1 and RB1 cores (purple circles). The background is a 5-m cell DTM (modified from data provided by Regione Veneto, 2011), stretched to highlight elevation changes. Scarps bounding the post-glacial incision of the Brenta megafan are evidenced with black dashed lines.

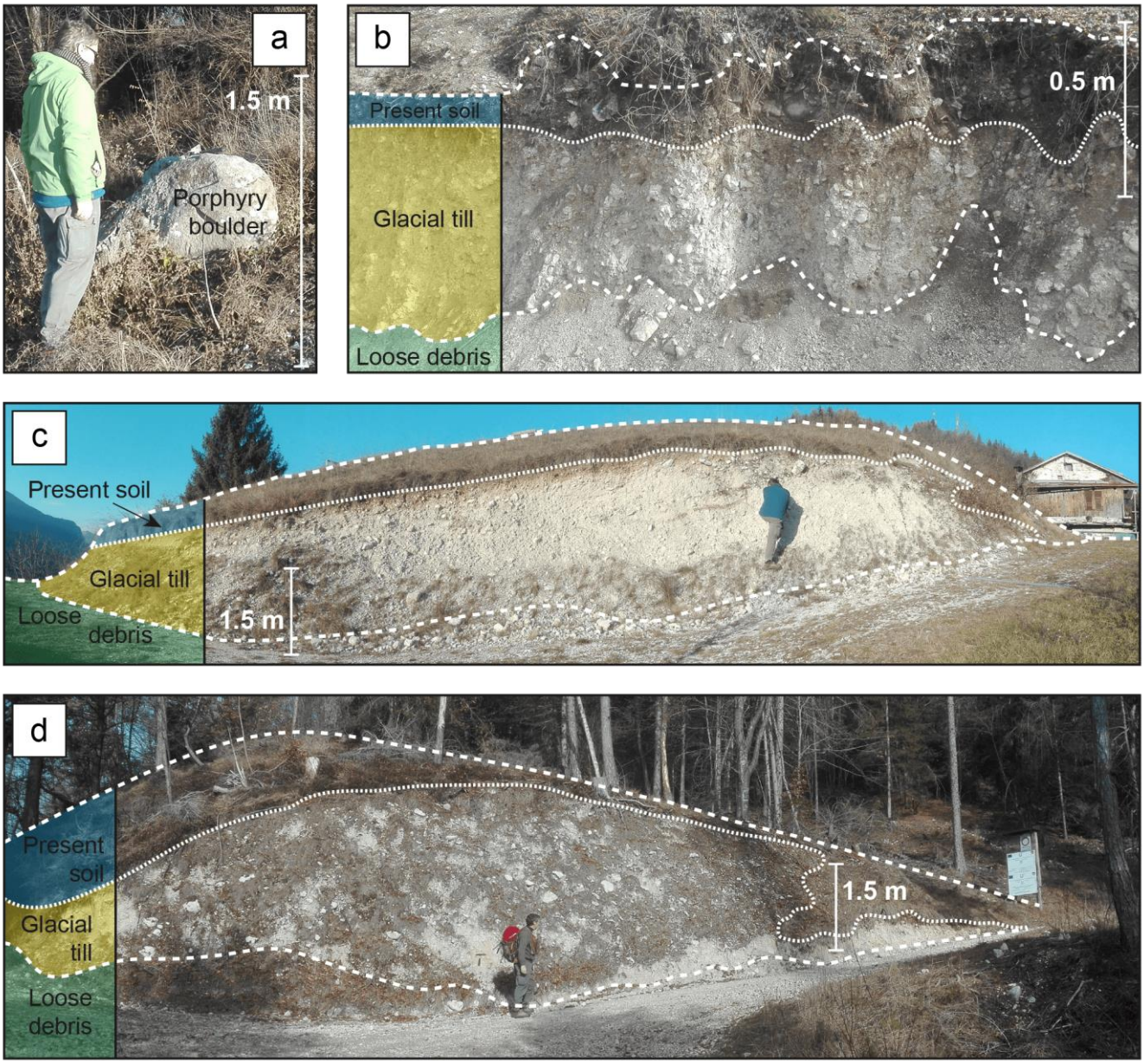

Figure 4: Photos taken in the middle sector of the Valsugana valley. When present, stratigraphic layers are separated by dotted/dashed white lines. a) porphyry boulder, located on top of Col del Gallo mount; b) section of a lateral moraine of the Brenta glacier, located on top of the Novegno mount; c) moraine, located on the southern sides of Col del Gallo mount; d) moraine, located in the Sorist area.

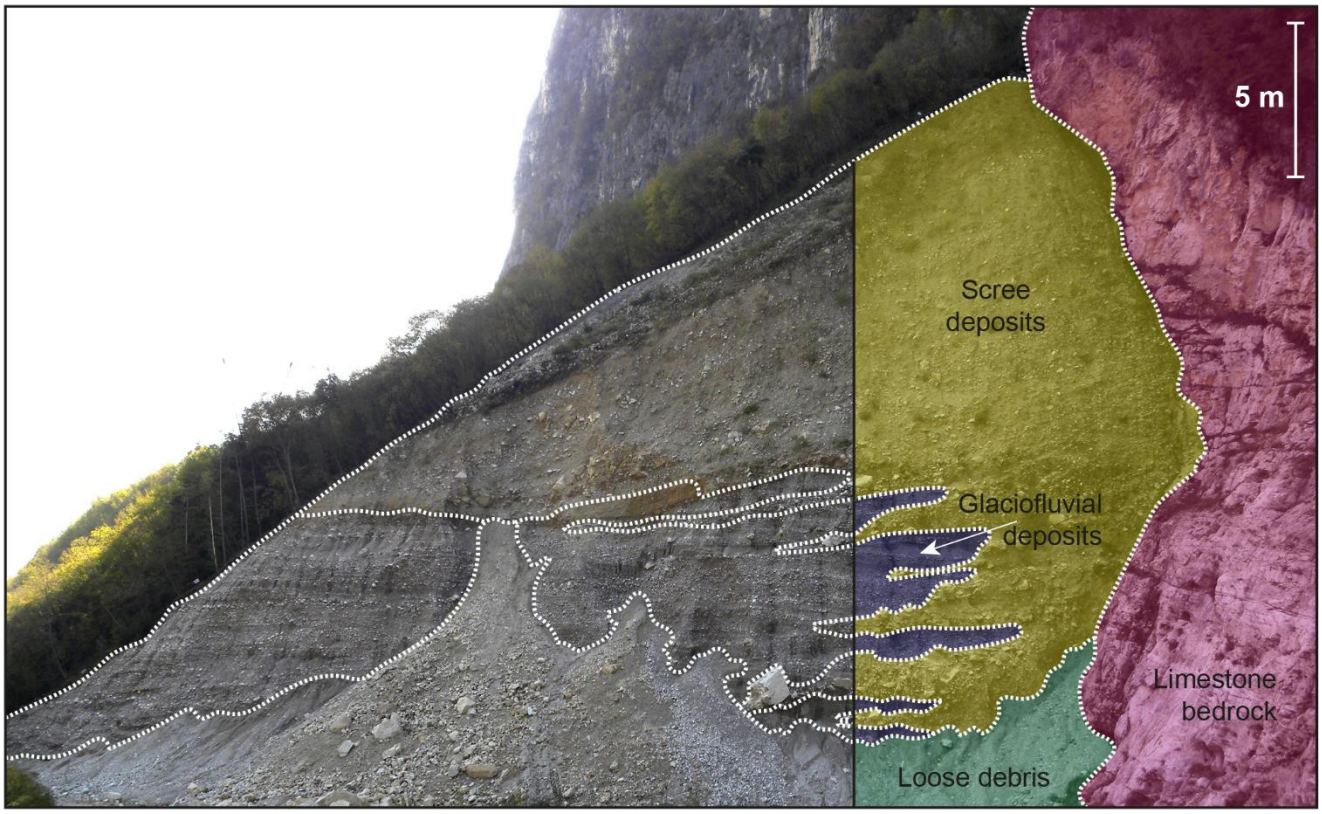

Figure 5: Coste section. It is possible to appreciate how inclined-bedding scree deposits overlie and interfinger with horizontal-bedding glaciofluvial sediments.

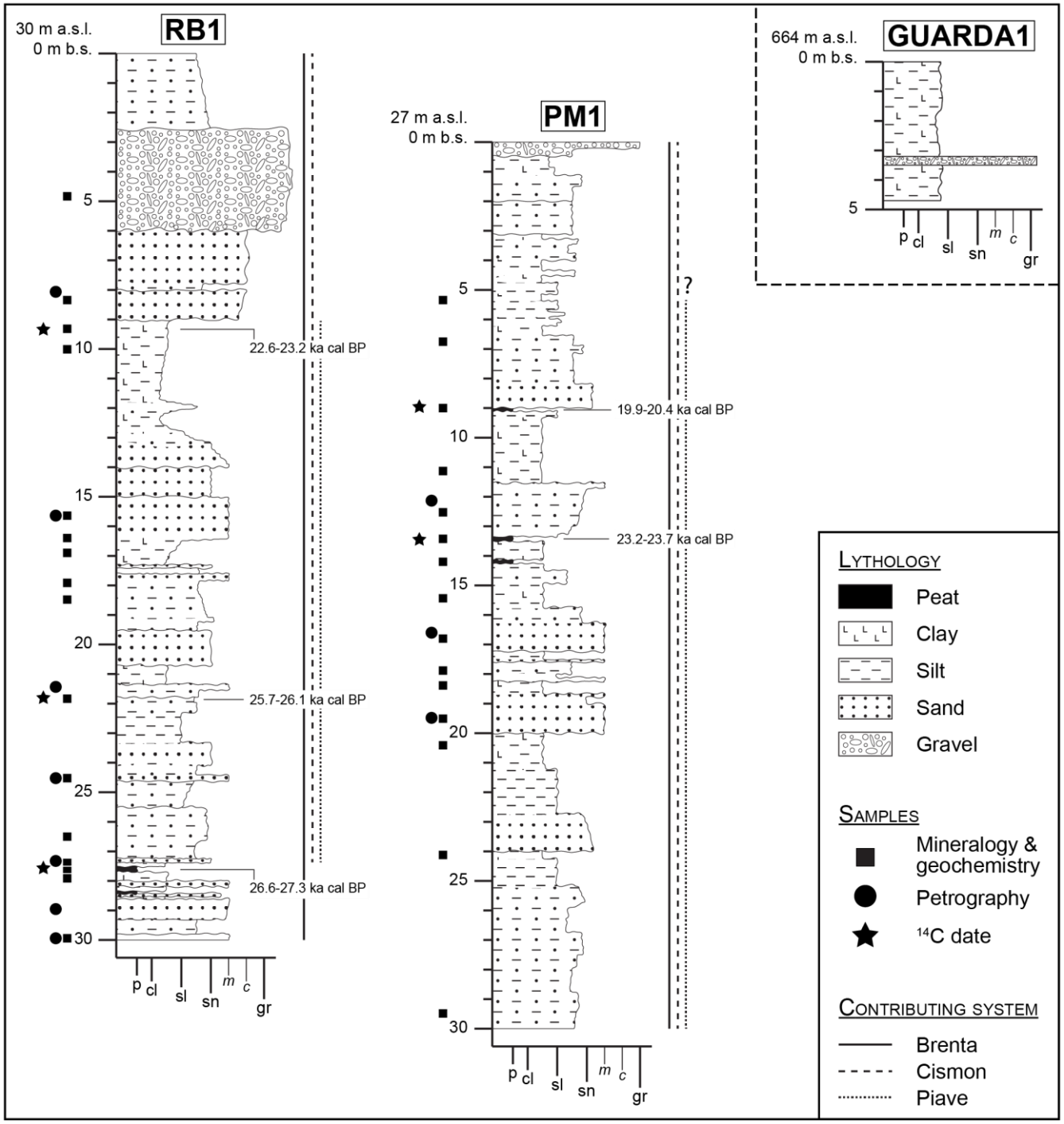

Figure 6: Stratigraphic logs of the RB1, PM1 and Guarda1 cores. Different catchments contributing to the sedimentation are marked by lateral solid/dashed lines. Samples are shown with different symbols according to the adopted technique.

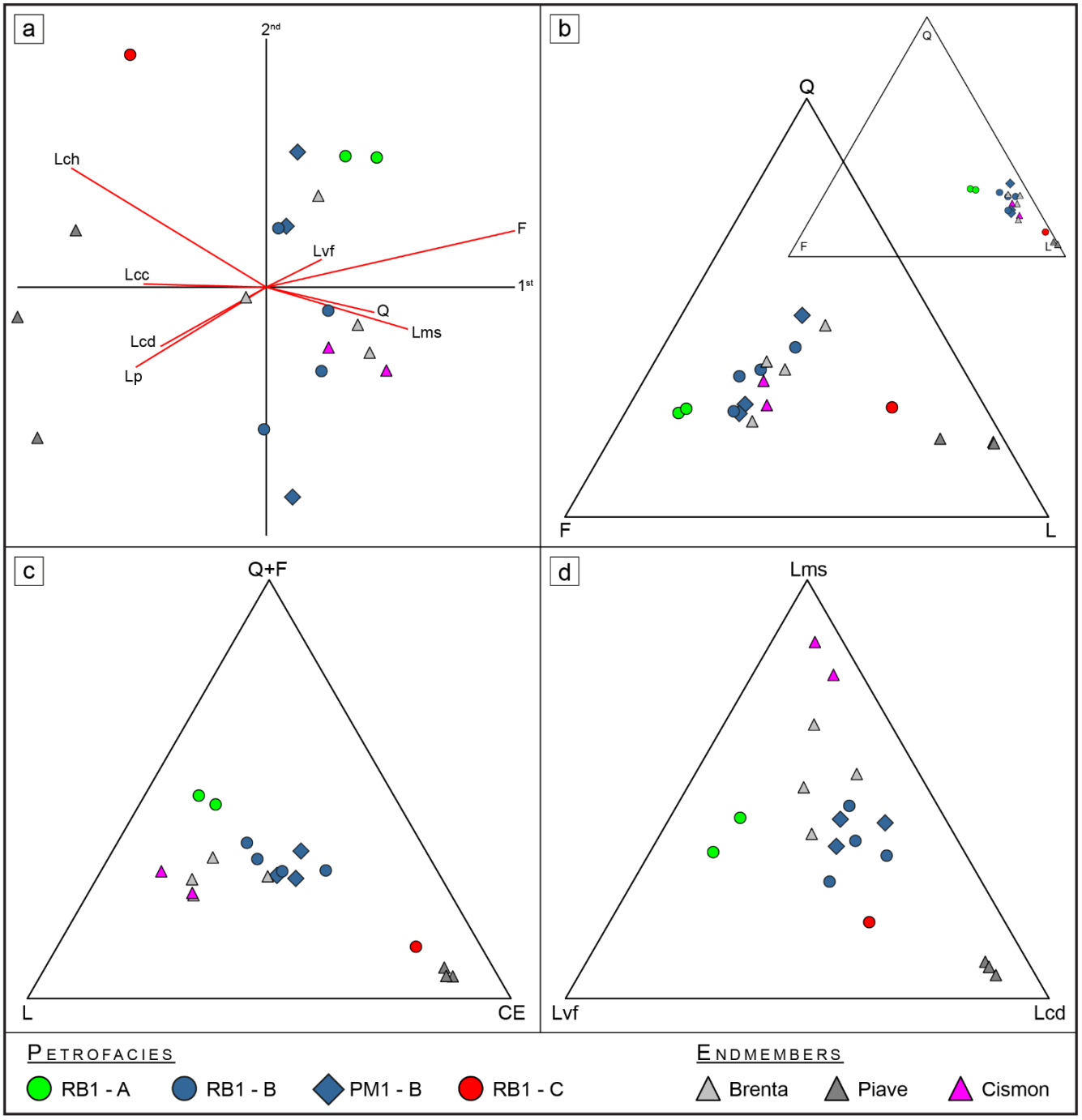

Figure 7: (a) Compositional biplot of the principal components; (b) original (small) and centred (large) QFL diagrams; (c) Q+F, L (non-carbonate lithic) and CE (carbonate lithic and cherts) and (d) Lms, Lvf and Lcd ternary diagrams with the results of the sand petrography analysis performed in RB1 and PM1 cores. Endmembers after Garzanti et al. (2006) and Monegato et al. (2010). See Table 2 for component acronyms.

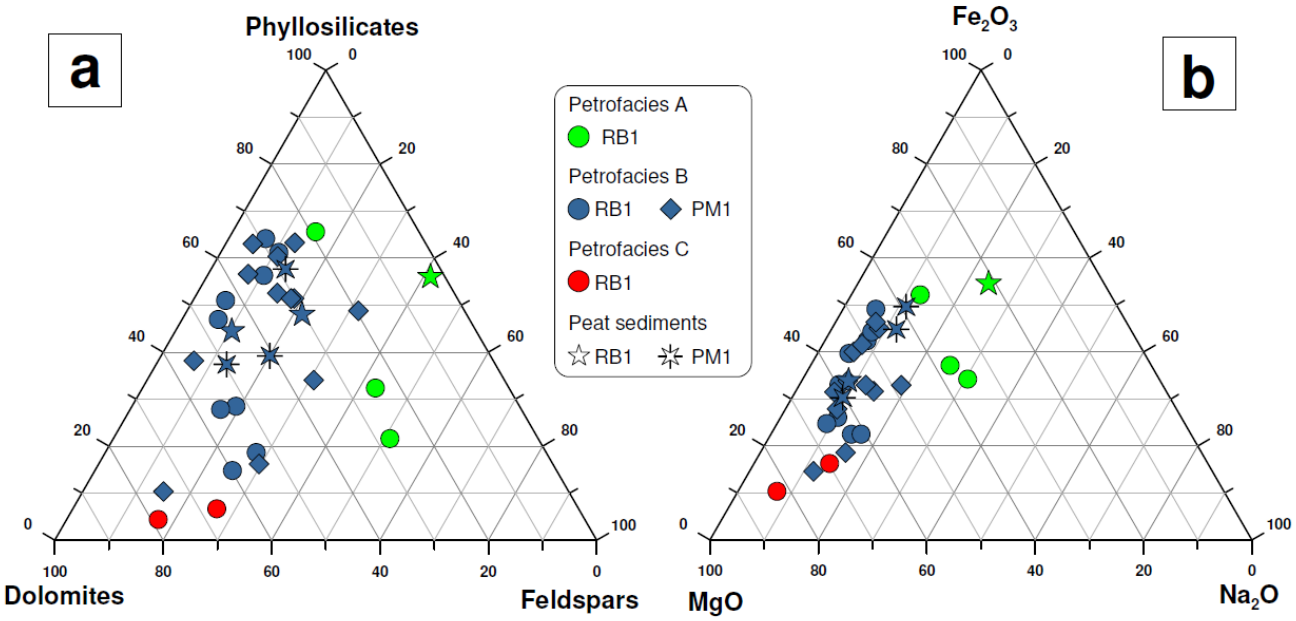

Figure 8: Ternary diagram reporting main selected mineral components (a) and geochemical components (b) of bulk sediments in RB1 and PM1 cores. Peat samples are evidenced with different symbols.

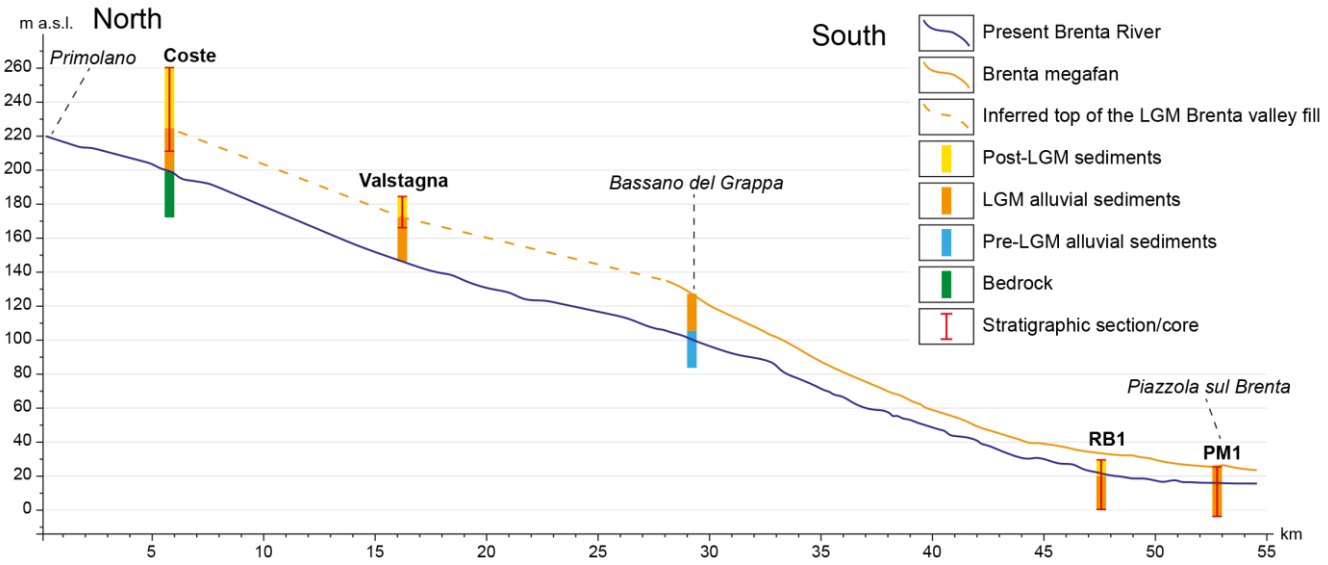

Figure 9: Longitudinal profiles of the present Brenta river (blue solid line), from Primolano to Piazzola sul Brenta, the Brenta megafan (orange solid line), from the apex to Piazzola sul Brenta, and the possible profile of the Brenta valley bottom during LGM (orange dashed line), inferred from stratigraphic sections. The age of sediments/bedrock is shown with different colours.

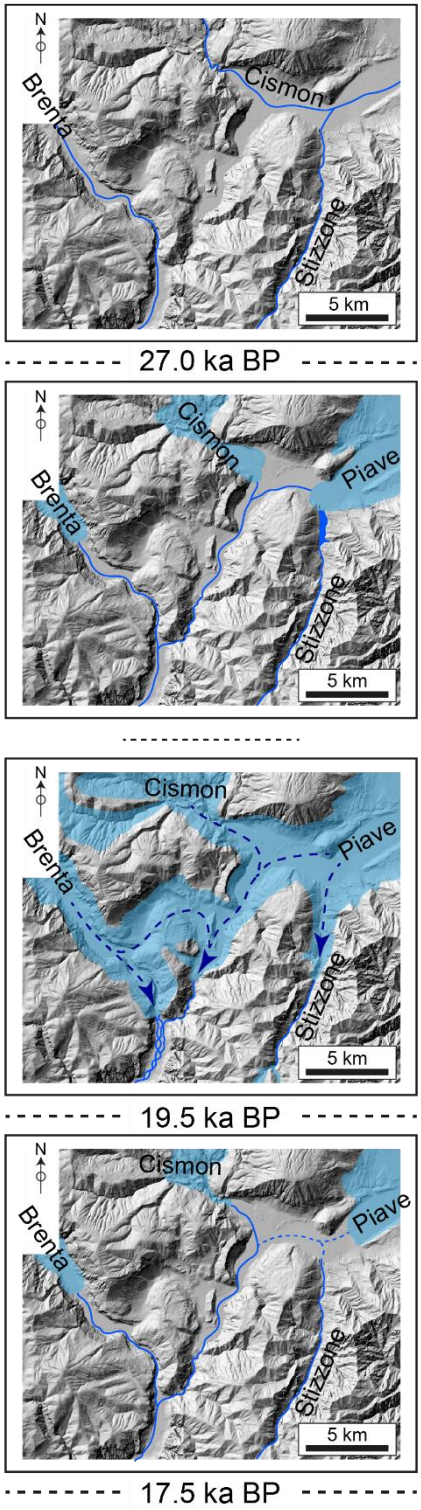

Figure 10: Evolution of the middle sector of the Valsugana valley since the onset of LGM; see text for details.

Sample name	Lab. code	Material	Depth [m]	Thickness [cm]	Uncalibrated age [years BP]		Calibrated age (IntCal 13 - 2σ) [years BP]		
					Lab. age	Uncertainty (±)	Min	Max	Median prob.
PM1-1	UZ-6073	Peat	9.00	1.5	16,700	60	19,945	20,362	20,147
PM1-2	UZ-6074	Peat	13.45	1	19,500	75	23,167	23,754	23,495
RB1-1	UZ-6075	Peat	9.30	1.5	19,050	70	22,648	23,221	22,938
RB1-2	UZ-6076	Peat	21.80	1	21,610	90	25,715	26,058	25,888
RB1-3	UZ-6077	Peat	27.50	1	22,660	90	26,634	27,296	27,013

Table 1: Conventional, calibrated and median probability ^{14}C ages obtained from samples collected on RB1 and PM1 cores. Calibration was made with OxCal (version 4.2, Bronk Ramsey, 2009), based on the IntCal13 calibration curve (Reimer et al., 2013).

Sample	Depth [m]	Q	F	Lvf	Lvi	Lvp	Lcc	Lcd	Lp	Lch	Lms	Lmi	tot	Contribution of endmembers (R^2)
PM1-12	12.1	30.5	4.7	6		0.5	14.4	20.8	3.5	0.2	19.4		100	50%Brenta, 20%Cismon, 30%Piave (**0.76**)
PM1-17	16.6	18.2	10.6	9.1	0.3	2.6	23.9	14.8	1.4	1.1	17.9	0.3	100	30%Brenta, 20%Cismon, 50%Piave (**0.80**)
PM1-19	19.4	19.5	9.9	13.1		2.1	15.5	19.3	0.6	1.6	18.4		100	50%Brenta, 20%Cismon, 30%Piave (**0.93**)
RB1-8	7.9	10.3	2.1	8		0.3	47.3	15.3	1.6	10.1	5.2		100	All combinations (<**0.7**)
RB1-16	15.7	25.1	5.5	7.5			18.9	22.5	4.6	0.5	15.5		100	40%Brenta, 10%Cismon, 50%Piave (**0.79**)
RB1-21	21.4	26.8	10.4	9.7		1.7	5.6	18.9	1.6	0.7	24.4	0.2	100	50%Brenta, 30%Cismon, 20%Piave (**0.88**)
RB1-24	24.45	19.3	11.1	11.1		1.1	12	21.6	2.2	1.8	19.7	0.2	100	50%Brenta, 20%Cismon, 30%Piave (**0.93**)
RB1-27	27.3	25.1	8.3	18.8	0.3		3.3	24.3	2.8	0.5	16		100	80%Brenta, 10%Cismon, 10%Piave (**0.94**)
RB1-29	28.95	28.3	20.2	19.2		1.5	2.5	6.6	1.1	1	19.2		100	100%Brenta (**0.83**)
RB1-30	29.95	27.9	18.5	21.1		2.6	7.8	5.3	0.3	1	14.1		100	100%Brenta (**0.83**)

Table 2: Detrital modes of the sand fraction collected on RB1 and PM1 cores. List of acronyms: Q: quartz; F: feldspars; Lvf: felsic volcanic and subvolcanic lithic fragments; Lvi: intermediate and mafic lithic fragments; Lvp: plutonic lithic fragments; Lcc: limestone grains; Lcd: dolostone grains; Lp: shale, siltstone lithic fragments; Lch: chert grains; Lms: low-grade metamorphic lithic fragments; Lmi: medium-grade metamorphic lithic fragments.

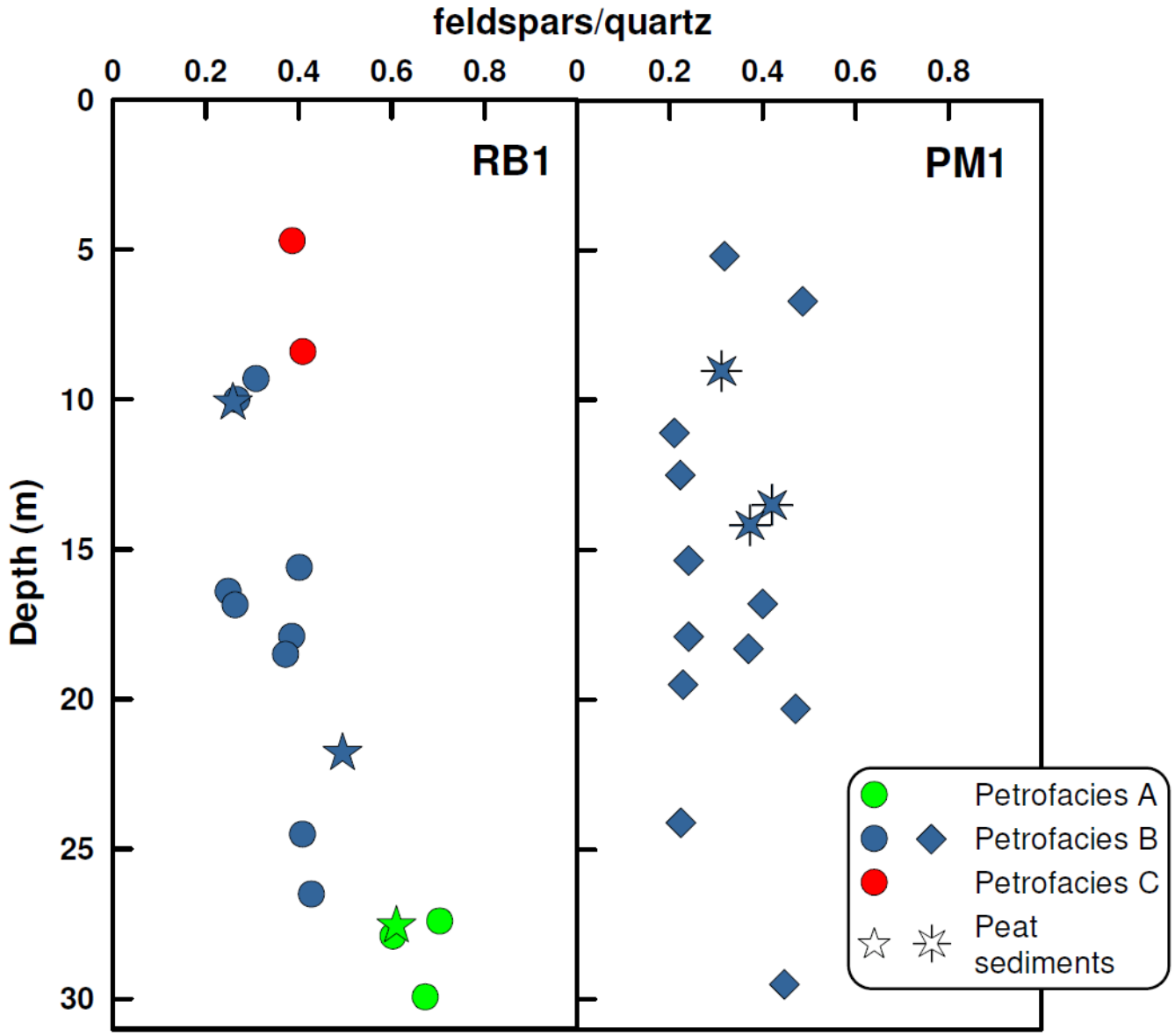

SFigure 1: Feldspars/quartz ratio in RB1 and PM1 cores (bulk sediments). This mineralogical parameter is useful to highlight peculiar compositional features of petrofacies A, B and C.

RB1 core	1	2	3	4	5	6	7	8	9	10	11	12	13	14	15	16	17	A
Depth (m)	0.5	4.7	8.4	9.3	10.0	10.1	15.6	16.4	16.9	17.9	18.5	24.5	26.5	27.4	27.6	27.9	29.9	21.85
Mineralogial analyses (wt%)																		
Quartz	21	35	17	19	14	18	33	14	12	37	19	28	26	15	25	41	39	27
Calcite	6	15	37	12	25	20	15	31	30	12	6	5	5	10	1	2	5	3
Dolomites	21	34	32	15	16	19	31	25	22	27	22	31	37	13	1	14	14	19
Plagioclase	6	10	5	4	3	4	11	3	2	12	6	9	10	10	13	20	19	10
K-feldspar	1	4	2	1	1	<1	2	1	1	3	1	3	2	1	3	5	7	3
Phyllosilicates	33	3	2	33	36	18	8	25	26	10	38	17	19	45	21	19	11	29
Am.XRD	14	<1	5	16	4	20	<1	1	7	<1	8	7	2	6	36	<1	4	9
Chemical analyses (wt%)																		
SiO2	40.65	45.17	23.97	37.94	32.77	30.81	44.13	28.88	27.34	49.21	39.58	43.50	39.15	42.14	45.90	59.94	61.30	
TiO2	0.64	0.14	0.10	0.39	0.39	0.30	0.23	0.23	0.31	0.21	0.30	0.29	0.26	0.41	0.45	0.53	0.28	
Al2O3	14.00	5.62	3.29	13.19	12.96	8.96	6.23	8.33	9.64	7.25	14.62	9.13	8.95	16.18	11.84	12.40	10.94	
Fe2O3 tot	5.03	1.25	0.75	4.17	4.72	2.82	1.90	2.92	3.99	1.82	5.36	2.95	2.93	5.67	3.45	3.13	2.43	
MnO	0.13	0.02	0.02	0.06	0.09	0.04	0.04	0.06	0.08	0.03	0.08	0.04	0.05	0.11	0.04	0.04	0.03	
MgO	5.30	5.36	5.97	4.90	4.31	4.79	5.29	5.26	5.48	4.92	5.81	7.17	7.82	3.82	1.35	3.13	2.51	
CaO	10.79	19.54	32.44	12.50	18.70	18.48	19.22	24.23	24.18	15.62	12.22	13.74	15.83	11.34	2.21	6.47	8.03	
Na2O	0.92	1.07	0.52	0.76	0.58	0.72	1.25	0.64	0.58	1.34	0.93	1.19	1.08	1.38	1.53	2.17	2.16	
K2O	2.73	1.47	0.71	2.92	2.87	1.94	1.45	1.82	2.16	1.88	3.50	2.21	2.14	3.55	2.49	2.95	2.85	
P2O5	0.17	0.05	0.04	0.11	0.10	0.11	0.07	0.11	0.11	0.07	0.13	0.09	0.09	0.15	0.16	0.10	0.09	
L.O.I.	*19.04*	*20.51*	*31.89*	*22.63*	*22.15*	*31.27*	*20.23*	*27.35*	*26.51*	*17.45*	*17.35*	*19.55*	*21.32*	*15.16*	*30.42*	*8.68*	*9.49*	
Tot	99.40	100.20	99.70	99.58	99.64	100.24	100.04	99.83	100.38	99.80	99.88	99.86	99.62	99.91	99.84	99.53	100.11	
N (%)	0.15			0.14		0.33			0.03						0.76			
Corg (%)	1.28			3.18		5.62			0.40						14.70			
ppm																		
As	32	20	1	55	23	84	18	19	11	0	<1	12	2	20	103	20	4.6	
Cd	2.9	0	0	0	0	1	0	<1	0	0	1	0	0	2	2	0	0	
Cr	80	19	8	47	28	72	8	38	34	11	82	23	37	79	61	51	20	
Cu	34	6	1	21	6	30	5	19	9	2	29	5	19	33	25	10	7	
Ni	35	3	3	44	14	31	4	22	15	9	25	6	17	29	17	40	18	
Sr	92	138	155	144	159	160	82	139	123	68	100	71	69	83	69	96	82	
Zn	114	127	18	84	78	227	44	67	57	28	121	37	2	132	51	77	58	

PM1 core	A	B	C	D	E	F	G	H	I	L	M	N	O	P	Q
Depth (m)	5.2	6.7	9.0	11.1	12.5	13.5	14.2	15.4	16.8	17.9	18.3	19.5	20.3	24.1	29.5
Mineralogial analyses (wt%)															
Quartz	17	28	22	15	29	14	18	12	31	17	15	33	13	15	35
Calcite	19	11	1	22	17	0	0	27	16	35	31	15	30	1	2
Dolomites	14	8	26	26	11	12	13	14	23	9	10	38	25	21	18
Plagioclase	5	12	6	3	5	5	5	2	9	3	5	7	2	3	11
K-feldspar	0	2	1	0	2	1	1	1	3	1	0	1	0	0	5
Phyllosilicates	29	21	20	18	18	25	13	22	7	15	27	5	18	42	17
Am.XRD	15	19	25	16	18	43	49	22	11	20	12	1	12	17	12
Chemical analyses (wt%)															
SiO2	37.84	47.85	36.44	30.89	42.21	35.91	29.75	29.15	44.75	27.94	30.04	42.39	29.12	39.09	54.13
TiO2	0.29	0.24	0.26	0.23	0.24	0.35	0.27	0.26	0.18	0.22	0.25	0.17	0.26	0.30	0.36
Al2O3	11.63	9.43	9.38	8.88	8.83	12.86	8.90	10.59	5.27	6.27	9.83	4.84	9.77	15.42	11.23
Fe2O3 tot	4.05	2.79	2.78	2.88	3.01	4.15	2.81	3.94	1.29	1.93	3.01	1.21	3.57	4.91	3.03
MnO	0.07	0.05	0.03	0.05	0.06	0.04	0.03	0.07	0.03	0.04	0.06	0.03	0.06	0.07	0.05
MgO	4.16	4.76	5.54	5.61	5.00	3.26	2.71	3.93	4.56	4.34	5.11	6.11	4.77	6.04	4.44
CaO	16.95	14.48	10.65	22.42	17.65	4.95	5.05	23.73	19.51	25.48	22.95	19.35	23.98	10.20	9.99
Na2O	0.78	1.27	0.86	0.66	1.12	0.95	0.75	0.63	1.09	0.66	0.75	0.98	0.58	0.86	1.73
K2O	2.66	2.08	1.85	1.91	1.79	2.56	1.54	2.29	1.37	1.33	2.16	1.18	2.08	3.43	2.39
P2O5	0.15	0.18	0.24	0.23	0.21	0.18	0.30	0.36	0.19	0.28	0.20	0.22	0.20	0.18	0.09
L.O.I.	*21.02*	*16.77*	*31.94*	*26.11*	*19.91*	*34.39*	*47.59*	*24.81*	*21.31*	*31.11*	*25.35*	*23.34*	*25.65*	*19.49*	*12.47*
Tot	99.60	99.90	99.97	99.87	100.03	99.60	99.70	99.76	99.55	99.60	99.71	99.82	100.04	99.99	99.91
N (%)			0.38			0.64	1.13			0.24				0.14	
Corg (%)			7.25			14.46	21.90			3.04				1.75	
ppm															
As	4	35	87	15	6	181	220	15	23	27	19	31	20	60	13
Cd	6	3	5	5	6	10	12	7	13	8	3	8	14	11	10
Cr	54	29	39	44	33	55	69	66	16	34	46	22	58	69	53
Cu	30	24	26	22	23	27	32	25	31	21	22	12	20	37	24
Ni	25	33	24	21	28	18	18	15	16	12	13	8	9	6	2
Sr	194	119	80	170	174	82	80	241	130	206	199	109	264	89	132
Zn	228	135	132	130	268	142	164	153	143	127	180	111	133	267	263

STable 1: Results of mineralogical and geochemical analyses of RB1 and PM1 cores.